97-112

Environment Canada
Water Science and Technology Directorate

Direction générale des sciences et de la technologie, eau
Environnement Canada

Groundwater flow and solute transport in fractured media

By:

P. Lapcevic, K. Novakowski, E. Sudicky

97-112

MANAGEMENT PERSPECTIVE

Title: Groundwater Flow and Solute Transport in Fractured Media

Author(s): P.A. Lapcevic, K.S. Novakowski and E.A. Sudicky

NWRI Publication #: 97-112

Citation: Chapter 16,"The Handbook of Groundwater Engineering", CRC Press Inc., expected publication Fall 1997.

EC Priority/Issue:

This chapter represents a compilation of our expertise in field and modelling techniques used to characterize groundwater flow and solute transport in fractured rock. The chapter was written as a means of disseminating our technical expertise in this field. The document will provide a reference document for future students and colleagues with little or no experience in the hydrogeological characterization of fractures in rock deposits.

Current Status:

The chapter has been submitted to CRC Press and is currently undergoing review by two external professionals. Besides revisions for publication, no other work is expected to be undertaken on this project. The development of improved field and modelling techniques to characterize fractured rock systems is an integral part of all our research studies.

Next Steps:

We are currently awaiting review of the document. The nature of this document is such that no further work is expected on it.

17

Groundwater Flow and Solute Transport in Fractured Media

P. A. Lapcevic and
K. S. Novakowski
National Water Research Institute
Burlington, Ontario

E.A. Sudicky
University of Waterloo

17.1 Introduction

Many of the world's largest aquifers reside in fractured consolidated media. Studies have shown that even media traditionally considered to be of low permeability, such as shales and granites, are fractured to the extent that significant groundwater flow may occur. In North America, there are many locales at which bedrock of either sedimentary or crystalline origin is used for either domestic or commercial water supply. In many geological settings, the lack of a protective layer of low-permeability clays or clay tills makes these water supplies particularly vulnerable to groundwater contamination.

Understanding groundwater flow in fractured consolidated media has long been important when undertaking engineering tasks such as dam construction, mine development, the abstraction of petroleum, slope stabilization, and the construction of foundations. To study groundwater flow in support of these tasks, often only relatively simple measurements of permeability conducted *in situ* are required. More recently, the discovery of groundwater contamination in fractured bedrock materials has led to the

0-8493-2698-2/99/$0.00+$.50

advent of many new investigative techniques that are quite different from those previously used in the geotechnical and petroleum industries. In particular, the focus of most hydrogeological investigations has been on the characterization of the transport properties of the higher-permeability fractures in the rock mass.

On many occasions, groundwater investigations benefit from the development of a numerical model which is used to simulate the flow system. However, because groundwater flow is primarily governed by discrete fractures at the local scale, traditional mathematical methods, in which it is assumed that the hydrogeological properties vary in a smooth and continuous fashion (a single continuum), provide a poor approximation. Only at large, regional scales of groundwater flow or where fracturing is very dense might continuum methods be applied in fractured media. Further, the often complex and heterogeneous arrangement of discrete fractures makes for difficulties in the representation of these features on an individual basis. There are several modeling approaches that can be used to circumvent this problem, including the use of stochastic or mixed deterministic-stochastic techniques (e.g., Smith and Schwartz, 1984) and the use of scale-dependent multicontinua (e.g., Bear, 1993). However, numerical models which can represent two-dimensional groundwater flow and solute transport in each discrete fracture within a three-dimensional randomly fractured domain of practical size have yet to be applied. Because it is impossible to characterize a field site to the degree necessary to support this type of model, a compromise such as the alternate approaches suggested above will almost always be required.

In this chapter, we will try to provide basic theory and practical advice for guiding investigations of the hydrogeology of fractured rock sites. Our aim has been to focus this discussion on the hydrogeological representation of fractured rock systems at scales below which an equivalent porous media (EPM) approach is adequate. To this end, the modeling and field sections will outline techniques to characterize discrete fractures and fracture networks in the subsurface. A basic introduction to structural geology will be provided to assist in determining how the features that govern groundwater flow in fractured media are formed and how to go about finding them. A brief outline of the principal processes involved in the flow of groundwater and transport of contaminants in individual fractures is presented. In addition, some methods commonly used in the field characterization of fractured rock will be described. These elements become the building blocks for the development of a conceptual model of groundwater flow. A discussion of conceptual models for both single fractures and fracture networks is included. Finally, an overview of analytical and numerical modeling techniques for fractured rock will be presented.

17.2 Structural Geology of Fractured Rock

In this chapter, the term fracture is used to refer to any discontinuity in a solid material. In geological terms, a fracture is any planar or curviplanar discontinuity that has formed as a result of a process of brittle deformation in the earth's crust (Engelder et al., 1993).

Planes of weakness in rock respond to changing stresses in the earth's crust by fracturing in one or more different ways depending on the direction of the maximum stress and the rock type. Three broad types of fractures have been identified based on the motion involved in the formation of the fracture. Opening mode (mode I) cracks form by the separation of the crack walls, under the action of tensile stresses normal to the crack plane (Figure 17.1a). Mode I fractures are thus extension fractures in which the fracture walls have displaced normal to the crack plane and no appreciable displacement parallel to the fracture plane has occurred. Sliding mode (mode II) cracks propagate by mutual shearing of the crack walls with the shearing oriented in the direction normal to the crack front (Figure 17.1b). Tearing mode (mode III) cracks advance when the crack walls are subject to a shearing aligned parallel to the crack front (Figure 17.1c). Mode II and III fractures are defined as shear fractures.

Joints (mode I fractures) are the most common type of fracture structure and are found in all types of rocks as well as in partly consolidated to unconsolidated sediments. Joint sets are characterized as systematic or nonsystematic. Joints belonging to a set maintaining consistent characteristics such as orientation, morphology, mineralization, and distribution between outcrops in a local and regional scale

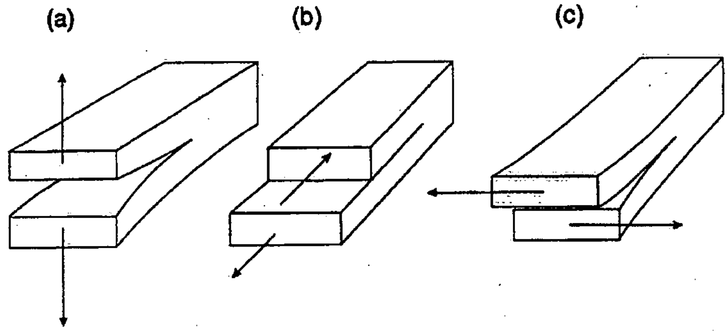

FIGURE 17.1 Schematic diagram showing mechanism of fracture formation: (a) Mode I (opening), (b) Mode II (sliding), (c) Mode III (tearing). (From Atkinson, B. K. 1987. *Fracture Mechanics of Rock.* Academic Press, Orlando, FL. With permission.)

are defined as systematic (Engelder et al., 1993). Nonsystematic joints have highly curved and irregular fracture surfaces and are not easily related to a recognizable stress field.

Groundwater movement in fractured rock depends on discontinuities at a variety of scales ranging from microcracks (micrometers, μm, in length and width) to faults (kms in length and meters in width). Fracturing in a large-scale rock mass can be loosely classified on the basis of three scales of discontinuity: (1) microscopic, (2) mesoscopic, and (3) megascopic.

At the microscopic scale, isolated or continuous disc-shaped microcracks ranging in length from 100 to 1000 μm and 1 to 2 μm in width are common to both crystalline and sedimentary rocks. Microcracks are normally mode I fractures, and often form in a disc-shape. In some cases, particularly adjacent to shear fractures, microcracks may form under mode II conditions.

In crystalline rocks, the total porosity of the rock matrix (i.e., the rock bounded by macroscale fractures) is due to microcracks and may range from 0.01% to 1.0%. In sedimentary rock, in addition to microcracks, significant porosity in the matrix may also occur due to incomplete cementation, the weathering of vugs, or imperfect lattice development. Matrix porosity in sedimentary rock may range from less than 1% to 50%.

At the mesoscopic scale, fractures (or joints) ranging between <0.5 m and >1000 m in length with widths ranging from <10 μm to >10 mm predominate in the groundwater flow system. These fractures are often grouped in sets having similar orientation which are related to the mode of fracture genesis. Fracture zones at this scale are defined as sets of closely spaced fractures contained within a narrow band. Shear fractures are also observed at this scale. A common and extremely important class of fractures at this scale is known as sheeting structure (Holzhauser, 1989). Sheeting structure forms due to the vertical expansion of the rock resulting from erosional unloading. Sheeting structures are present in all types of rock, often found parallel to the earth's surface, and are common conduits for groundwater flow at the regional scale. In plutonic and metamorphic rocks, they are often independent of the original macrostructure and fabric of the rock and are found at decreasing frequency with increasing depth (Trainer, 1988).

At the megascopic scale, faults and shear zones dominate the fracture morphology. A fault is defined as a planar discontinuity between two blocks of uniform rock where displacement has taken place parallel to the discontinuity. These are large-scale fractures with many associated features and may be either of high or low permeability depending on infilling and local stress fields. Faults may be of any orientation, although it is the sub-vertical features that are most easily identified through air-photo or map interpretation. Shear zones are similar to faults (i.e., a large-scale fracture zone which has undergone shearing) and are typically found in metamorphic terrain. These features are often of high permeability. In many fractured rock environments, the frequency and spacing of faults and shear zones are sparse. For example, Figure 17.2 illustrates in plane view the possible surface expression of a hypothetical distribution of

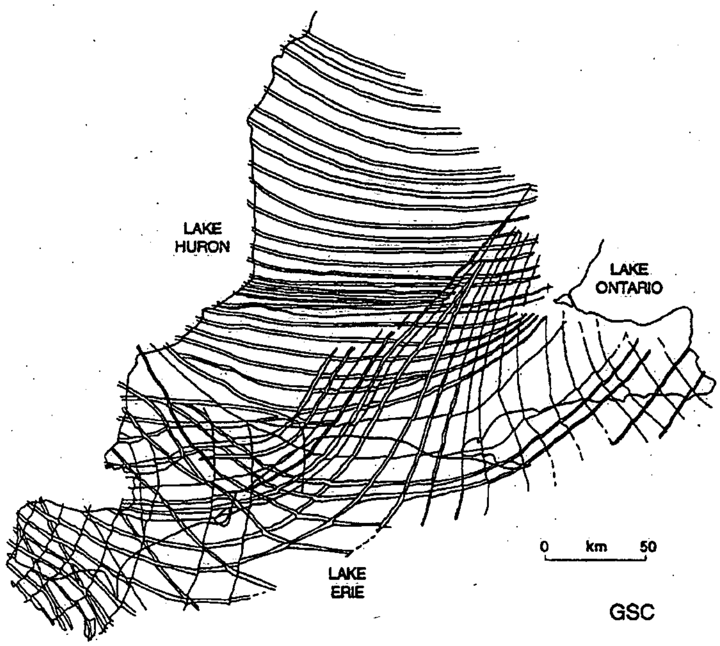

FIGURE 17.2 Distribution of regional faults in southern Ontario. (From Sanford, B. V., Thompson, F. J., and McFall, G. H. 1985. Phanerozoic and recent tectonics of the Canadian Craton, in *The Geoscience Program — Proceedings of the Seventeenth Information Meeting of the Nuclear Fuel Waste Management Program*, Atomic Energy of Canada Limited, TR-299:334-352. With permission.)

vertical faults in the southern Ontario region of central Canada. These faults are postulated to vertically penetrate the entire thickness of the sedimentary strata which ranges from ~200 m to ~2 km, in this area (Sanford et al., 1985). Note that the spacing between faults is several to tens of km. Thus, at the local to regional scale, any one of these faults may dominate the groundwater flow system.

Karst aquifer systems develop due to the extensive dissolution of fractured carbonate rock by flowing groundwater. The hydrogeology of this type of rock terrain is discussed in the following chapter.

17.3 Fundamentals of Groundwater Flow and Solute Transport in a Single Fracture

17.3.1 Groundwater Flow in a Single Fracture

Groundwater flow in a single fracture is often interpreted by assuming the fracture walls are analogous to parallel plates separated by a constant aperture. Using this analogy, solution of the Navier–Stokes equations for laminar flow of a viscous, incompressible fluid bounded by two smooth plates leads to an expression referred to as the cubic law. Figure 17.3 shows the parabolic distribution of velocity predicted by the solution to the Navier–Stokes equations in a cross section of a fracture having parallel walls. A rigorous mathematical development of the cubic law can be found in Bear (1972). Expressed as volumetric flow rate, Q, per unit drop in hydraulic head, Δh, the cubic law can be written as:

$$\frac{Q}{\Delta h} = C(2b)^3 \tag{1}$$

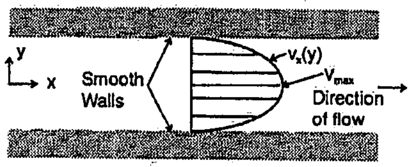

FIGURE 17.3 Schematic diagram showing parabolic distribution of velocity in a fracture having parallel walls.

where $2b$ is fracture aperture and C is a constant related to the properties of the fluid and the geometry of the flow domain. Thus, the flow rate is proportional to the cube of the aperture, hence the term cubic law. For straight uniform flow, the constant of proportionality is:

$$C = \frac{\rho g}{12\mu} \frac{W}{L} \tag{2}$$

where ρ is fluid density, g is acceleration of gravity, μ is kinematic viscosity, W is the width of the fracture, and L is the length of the fracture. For flow in radial domain, C is given as:

$$C = \frac{\rho g}{12\mu} \frac{2\pi}{\ln\left(r_e/r_w\right)} \tag{3}$$

where r_w is well radius and r_e is radius of influence. By substitution of the cubic law into Darcy's law, the transmissivity (T_{fr}) and hydraulic conductivity (K_{fr}) of a fracture can be defined:

$$T_{fr} = \frac{\rho g}{12\mu}(2b)^3 = K_{fr} 2b \tag{4}$$

Thus, using Equation (4) we can relate terms typically used to describe the permeability of a porous medium to that for discrete fractures.

Figure 17.4 illustrates for a range of hydraulic conductivities, the thickness of porous medium which would be equivalent to a single fracture of given aperture. For example, using Figure 17.4, we see that the volume of groundwater passing through a 10-m section of porous media having $K = 10^{-4}$ m/s is the same as can pass through a fracture less than 1 mm in width under the same driving force. Thus, even in sparsely fractured rock, considerable volumes of groundwater are moved about under typical hydraulic gradients.

The average groundwater velocity in a fracture can be found by combining Equation (4) and Darcy's law:

$$\bar{v} = -\frac{\rho g}{12\mu}(2b)^2 \frac{dh}{dx} \tag{5}$$

Groundwater velocities predicted using the cubic law over a range of hydraulic gradients are presented in Figure 17.5. Note that even for very small hydraulic gradients, groundwater velocity in discrete fractures is very high in comparison to velocities typical of porous media.

Where large hydraulic gradients are present, turbulent flow may occur. The transition from laminar to turbulent flow is estimated using the Reynolds number, R_e. For a planar fracture R_e is defined as:

$$R_e = \frac{\bar{v} D_h \rho}{\mu} \tag{6}$$

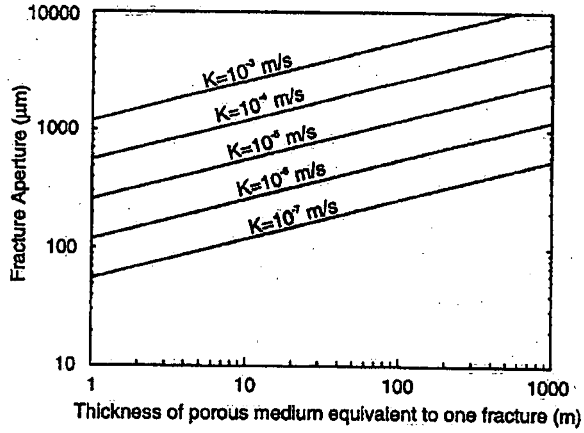

FIGURE 17.4 Comparison of aperture of a single fracture to equivalent thickness of porous media. (From de Marsily, G. 1986. *Quantitative Hydrogeology.* Academic Press, Orlando, FL. With permission.)

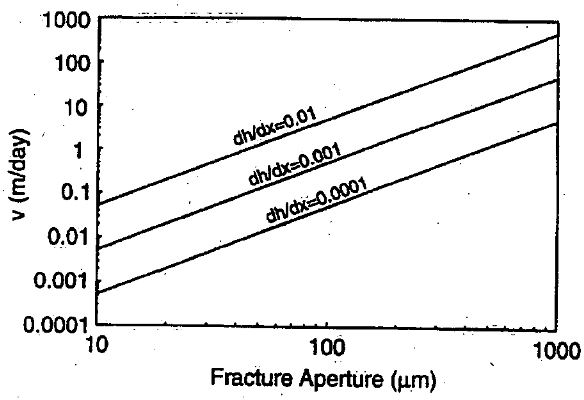

FIGURE 17.5 Groundwater velocity in a single fracture as predicted by the cubic law.

where $\bar{v}$ is mean velocity, and D_h is the hydraulic diameter. For planar fractures, D_h is defined as:

$$D_h = 2 \cdot 2b \tag{7}$$

In addition, the relative roughness of a fracture can be defined as:

$$R_r = \frac{\varepsilon}{D_h} \tag{8}$$

where ε is the mean height of the asperities (the peaks in the topographic surface of the fracture walls). The transition from smooth to rough flow occurs at an R_r of 0.033 and the transition from laminar to turbulent flow at a R_e of 2300 (de Marsily, 1986). Using R_r, the K_{fr} in a rough-laminar fracture can be expressed as:

$$K_{fr} = \frac{\rho g 2b^2}{12\mu\left(1 + 8.8R_r^{1.5}\right)} \tag{9}$$

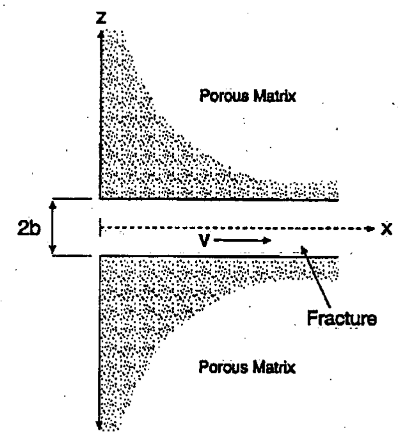

FIGURE 17.6 Schematic diagram of a single fracture in a porous rock.

Alternatively, the influence of fracture surface roughness can be incorporated directly into the cubic law by introducing a factor f that accounts for deviations from the ideal conditions that were assumed in Equation (1). In experimental studies using both radial and straight flow geometries and in fractures of various rock types having apertures ranging from 4 to 250 µm, f was observed to vary from 1.04 to 1.65 (Witherspoon et al., 1980). These results lead to a more generalized form of the cubic law:

$$\frac{Q}{\Delta h}=\frac{C}{f}(2b)^3 \tag{10}$$

where $f = 1$ for smooth walls and f is slightly greater than 1 for rough surfaces. Thus, predictions of groundwater flow based on the cubic law where $f = 1$ are generally adequate for most conditions.

17.3.2 Solute Transport in a Single Fracture

The transport of both conservative and reactive aqueous constituents in discrete fractures is governed by (1) hydrodynamic dispersion, (2)advection, (3) radioactive or biological decay, and (4) diffusion into the rock matrix. In addition, the transport of reactive compounds may be influenced by geochemical processes such as acid/base reactions, oxidation/reduction reactions, precipitation-dissolution, or adsorption-desorption.

The governing equation for solute transport in a single fracture (Figure 17.6) which incorporates advective transport, longitudinal dispersion, molecular diffusion from the fracture into the matrix, adsorption onto the face of the matrix, adsorption within the matrix, and radioactive decay is written as (Tang et al., 1981):

$$2b\left[R_a\frac{\partial c}{\partial t}+\bar{v}\frac{\partial c}{\partial x}-D_L\frac{\partial^2 c}{\partial x^2}+\lambda R_a c\right]+2q=0 \qquad 0\le x\le\infty \tag{11}$$

where the x-coordinate is in the direction of the fracture axis, C is the concentration of solute in the fracture, λ is a decay constant, and q is the diffusive flux perpendicular to the fracture axis. The retardation factor, R_a, is defined by:

$$R_a = 1 + \frac{K_{df}}{b} \tag{12}$$

where K_{df} is the distribution coefficient for the fracture walls defined as mass of solute adsorbed per unit area of surface divided by the concentration of solute in solution. To relate this to the distribution coefficient for the rock matrix, K_d, which is based on the bulk density of the material, an estimate of internal specific surface area of the medium, γ, is required. The specific surface area is defined as the area of the pore walls exposed to the fluid and has units of area per unit mass. Thus, the relation is given as:

$$K_d = \gamma K_{df} \tag{13}$$

The hydrodynamic dispersion coefficient, D_L, is defined following the standard formulation for porous media:

$$D_L = \alpha_L \bar{v} + D' \tag{14}$$

where α_L is the longitudinal dispersivity in the direction of the fracture axis and D' is the effective diffusion coefficient which incorporates the geometric effect of the pathways in the pore space. The governing equation for the matrix as derived by Tang et al. (1981) is:

$$\frac{\partial c'}{\partial t} - \frac{D'}{R'}\frac{\partial^2 c'}{\partial x^2} + \lambda c' = 0 \qquad b \le z \le \infty \tag{15}$$

assuming a single fracture penetrating an infinite medium where c' is concentration in the matrix, and the matrix retardation coefficient R' is defined as:

$$R' = 1 + \frac{\rho_b}{\theta_m} K_d \tag{16}$$

where ρ_b is the bulk density of the matrix, and θ_m is matrix porosity. The diffusive loss term q in Equation (11) represents diffusive mass flux crossing the fracture–matrix interface. Using Fick's first law, this can be expressed as:

$$q = -\theta_m D' \left.\frac{\partial c'}{\partial z}\right|_{z=b} \tag{17}$$

Thus, the final coupled equation for the fracture becomes:

$$2b\left[R_a \frac{\partial c}{\partial t} + \bar{v}\frac{\partial c}{\partial x} - D_L \frac{\partial^2 c}{\partial x^2} + \lambda R_a c\right] - 2\theta_m D' \left.\frac{\partial c'}{\partial z}\right|_{z=b} = 0 \qquad 0 \le x \le \infty \tag{18}$$

In porous and fractured rock, the loss of solute from the fractures into the rock matrix through the process of diffusion can be significant. To illustrate the effect of matrix diffusion, Figure 17.7 uses the solution to Equation (18) to show the relative concentration of solute in a single 500-μm fracture pervading a medium having a porosity of 1 to 10%. The velocity in the fracture ranges from 1 to 10 m/day and dispersivity is varied from 0.05 m to 0.5 m. Concentration input is continuous and the point of measurement is 50 m from the source. It is immediately evident that the effect of solute loss to the

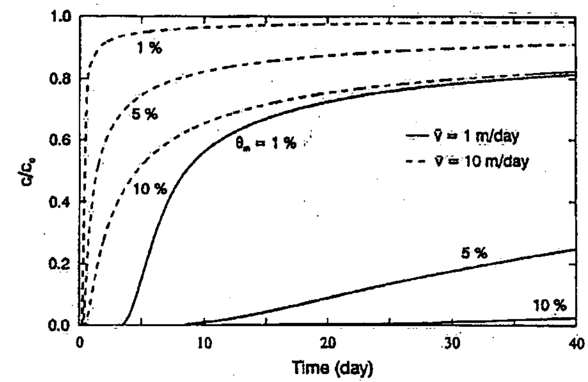

FIGURE 17.7 Concentration profiles in a 500-μm fracture, 50 m from a continuous source, illustrating the influence of matrix porosity on solute transport in a single fracture.

matrix is profound. The effect is so significant that the influence of hydrodynamic dispersion in the longitudinal spreading of solute is completely overwhelmed (i.e., different α_L results in little change in the shape of the curve).

17.4 Field Techniques

In order to develop a defensible conceptual model for a given flow system in fractured rock, some characterization of the medium is necessary. The degree of characterization is dependent on a variety of factors, including the inherent complexity of the fracture system (i.e., sedimentary versus crystalline rock), the type of conceptual model desired, and the amount of funding available. Because of the inherent heterogeneity of fractured rock masses (e.g., presence of sheeting structures), some characterization of the subsurface is essential in supporting conceptual models based only on surface measurements (i.e., fracture maps).

In the following, methods for the measurement of the surface and subsurface expression of fractures will be discussed. In addition, techniques for the measurement of the hydraulic parameters of both the fractures and unfractured matrix are discussed, and an overview of tracer methods used to measure solute transport parameters in fractured rock is presented. Finally, permanent multilevel borehole instrumentation specifically designed for fractured rock investigations is described. An essential component of comprehensive investigations of groundwater flow and solute transport in fractured media is the geochemistry of the groundwater. A discussion of groundwater geochemistry in fractured media, however, is beyond the scope of this chapter.

17.4.1 Fracture Mapping

To determine the distribution of systematic fractures, outcrops, quarry walls, pavements, or mine tunnels are mapped to estimate the strike, dip, and spacing of individual fractures. In practice, reference lines are established on the rock surface using a measuring tape oriented from north. The orientation, spacing, and trace length of all fractures intersecting these scanlines are measured. The bias introduced by the intersection of the fractures with an oriented scanline in this type of sampling must be considered during post-processing (La Pointe and Hudson, 1985). Other useful observations of the fractures on traces include the nature of the termination, mineralization, staining, and surface roughness. Qualitative observations of water or fluid seepage along fractures in road cuts or gorge faces can also be useful indicators of groundwater flow. It is important to note that in many cases surface fracture measurements will be reflective of near-surface stress conditions or may be influenced by the removal of the overlying rock in quarrying operations. Consequently, physical estimation of fracture aperture cannot reliably be con-

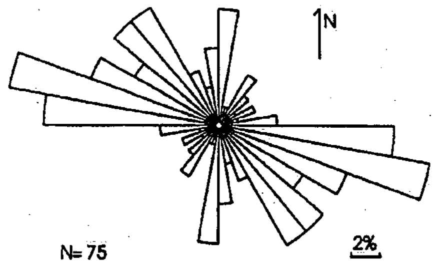

FIGURE 17.8 Rose diagram of orientations of vertical fractures intersecting seven boreholes to depths of 60 m in a flat-lying Silurian dolostone.

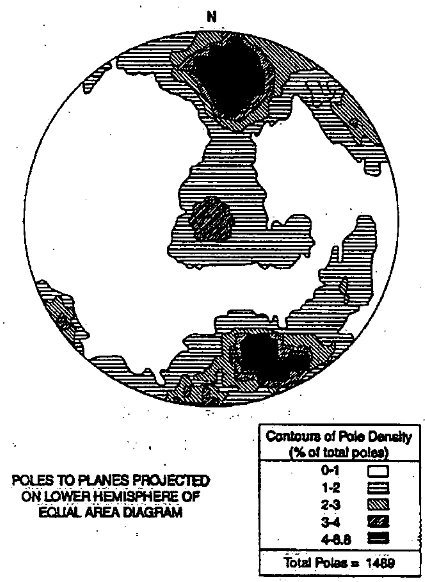

FIGURE 17.9 Equal area stereonet of fracture orientations plotted as poles to planes. (From Raven, K. G. 1986. Hydraulic characterization of a small ground-water flow system in fractured monzononitic gneiss. *Nat. Hyd. Res. Inst. Scientific Series No. 149*, No. 30, 133 pp. Government of Canada, Ottawa. With permission.)

ducted from surface measurements. In addition, due to the presence of sheeting structure, the fracture measurements obtained from surface exposures may not agree with those obtained *in situ*.

Measurements of fracture orientation are usually presented in one of two ways: (1) rose diagrams or (2) stereographic plots. Rose diagrams are histograms in which the frequency (usually as a percentage of total measurements) of joint orientations within 5 to 10° intervals are plotted by azimuth (Figure 17.8). Rose diagrams are commonly used in flat-lying sedimentary rock where most nonhorizontal fractures are vertical in orientation. In crystalline rock or deformed sedimentary rock with fracture sets of more random orientation, data are often presented as the projection of the poles of the planes (fractures) plotted (Figure 17.9) on equal-area stereonets (Ragan, 1973).

17.4.2 Core Analysis

Boreholes installed for groundwater investigations in fractured rock, using either percussion, tri-cone, or diamond drilling techniques, generally range in diameter from 48 mm to 152 mm. In North America, 76-mm or 96-mm diameter boreholes are generally drilled as test or monitoring wells, while 152 mm or greater diameter boreholes are used for water supply. Rock core obtained from diamond-drilled boreholes can be used to determine the subsurface pattern of fractures. While it is common to install only vertical boreholes, for most hydrogeological site investigations, installing boreholes in the inclined orientation will maximize the number of nonhorizontal and vertical fractures intersected. There is only nominal cost differential between inclined and vertical boreholes, and working in inclined boreholes is no more difficult than in vertical boreholes. In flat-lying sedimentary rock, inclined boreholes may be of better quality and less prone to blockages due to spalling rock.

The physical examination of rock core can be used to identify potentially open fractures through which groundwater flows. Natural fractures can be distinguished from mechanical breaks (breaks resulting from drill vibration, etc.) using the following criteria: (1) roughness of the fracture surface (wavy irregular fracture traces in natural fractures contrast to sharp, clean mechanically induced breaks), (2) presence of infilling (normally, calcite or sulfate mineralization), and (3) in crystalline or deformed sedimentary rock, evidence of shear or slickenside structure. Evidence of weathering or iron staining is indicative of groundwater flow. Examination of the core in detail for lithological changes is important, because discontinuities at geological contacts are frequently water-bearing fractures.

It is important to note that the aperture or width of naturally open fractures cannot be determined from physical measurements on the core. This is because removing core from the subsurface disrupts the natural stress conditions such that aperture values become arbitrary.

If the orientation of bedding is known or the core is oriented using an orientation device, it is a relatively simple procedure to obtain the orientation of nonhorizontal fractures by measuring the arc length of the fracture ellipse in the core (Lau, 1983). Orientation data may be displayed using the same methods as used for surface fractures. Fracture spacing from core can be determined as the spacing between naturally open fractures (eliminating all other fractures). Further details on the analysis of core, particularly in sedimentary rock, are discussed by Kulander et al. (1990).

17.4.3 Borehole Geophysical Methods

Borehole televiewer (BHTV) is one of the more useful borehole geophysical tools for determining the location and orientation of fractures in an open borehole (Zemanek et al., 1969). As the televiewer probe travels the borehole length, a rotating electronic transducer emits a pulsed ultrasonic beam. The reflection of this acoustic energy from the borehole wall produces an image which can be used to identify the strike, dip, and relative size of the fractures intersecting the borehole. The system characterizes fractures only in the immediate vicinity of the borehole. Additionally, it may be difficult to distinguish open fractures from the effects of drilling damage. BHTV surveys are carried out by relatively few groups worldwide and are usually expensive.

A borehole video camera (BVC) survey is a cost-effective alternative to BHTV, particularly for shallow boreholes (<100 m depth). BVCs film the borehole walls and produce either a color or black-and-white image of the borehole. Many of the cameras designed to inspect sewers or pipelines are easy to adapt to a borehole application. Automated depth counters allow for the location of specific features such as fractures, vugs, precipitates, mineralization, changes in lithology or the presence of flowing fractures. Mirrors can be attached to permit a side view of the borehole walls. A BVC survey conducted prior to hydraulic testing or the installation of permanent packer strings will reduce the chances of packer damage or zone leakage due to the inflation of packers over an enlarged portion of the borehole.

Recently, borehole temperature probes and borehole flow meters have been used to detect the presence of large, open fractures using either ambient flow in the borehole (Paillet and Kapucu, 1989) or pumping-induced vertical flow (Hess and Paillet, 1990). In both cases, these methods are sensitive only to the largest one or two fractures and provide little quantitative information about these features. Other geophysical logging tools suitable for fracture detection in open boreholes include: (1) two- or three-arm caliper, (2) formation microscanner, and (3) azimuthal laterlog. Conventional and imaging logs are compared for their ability to detect fractures in Jouanna (1993).

17.4.4 Hydraulic Testing Methods

The characterization of groundwater flow systems in fractured rock is generally dependent on measurements of the permeability of the rock (hydraulic testing). The principal aim of hydraulic testing is to determine the permeability of the fractures and of the rock mass to assist in the estimate of groundwater velocity through the fractures and to appraise groundwater resources. The key to successful field characterization of fractured rock systems lies in the design of hydraulic testing programs. This design should be developed from a preliminary conceptual model of the fracture framework and groundwater flow system. The choice of hydraulic test will depend on several factors including the expected permeability, fracture frequency, matrix properties, type of rock, depth of the borehole, inter-borehole spacing, and purpose of investigation. In this section, constant-head injection tests, and pulse interference testing will be described. In addition, some of the concepts important in the interpretation of hydraulic tests (i.e., wellbore storage and skin effects) will be introduced. A general description of various testing methods applicable to hydrogeological investigations in fractured rock can be found in Doe et al. (1987), and a comprehensive case study is provided by Raven (1986).

17.4.4.1 Hydraulic Testing Equipment

Essential equipment for testing the hydraulic properties of open boreholes in rock includes packers of some type and devices to measure pressure (i.e., pressure transducers). Packers are used to temporarily seal portions of an open borehole to allow for testing in specific zones. In some instances, hydraulic testing is carried out after the installation of permanent borehole instrumentation (discussed later in this section). Typically, for studies conducted at shallow depth (i.e., <100 m) in open boreholes, test zones may range from 2 to 10 m in length with packer seal lengths ranging from 1 to 2 m. In shallow systems, packers are normally inflated with compressed air or nitrogen. In deeper systems or in low-permeability rock, water can be used to provide a stiffer seal. Commercially available packers generally consist of a gland of rubber, steel-reinforced rubber, or neoprene over steel or PVC pipe with either a "fixed-head" or "sliding-head" design. Fixed-head packers rely on the stretch of the gland material during inflation to provide the seal. Conversely, with sliding-head packers, o-rings in the bottom head of the packer permit the gland to slide upward during inflation. This latter design allows for the use of stiffer (i.e., reinforced) materials to inflate against the borehole wall. The fixed-head design is adequate for shallow rock systems with competent borehole walls, while sliding-head packers are more suitable for use in deeper flow systems.

A two-packer system having a single isolated zone is usually adequate for hydraulic testing programs conducted in moderate to sparsely fractured rock. For conditions where fracture frequency is high and packer leakage or short circuiting effects around the main packers are anticipated, additional packers may be installed above and below the test section to monitor for these effects.

For multiwell testing, multiple-packer strings are normally used in the observation boreholes. In some cases, it may be convenient and cost-effective to install permanent packer strings in the observation boreholes (described later in this section).

The pressure response in the isolated source zone or in the observation zones to perturbations generated by injecting or withdrawing water from the source zone is usually measured using pressure transducers or transmitters. The most commonly used types of pressure transducers are based on either strain gauge or vibrating wire membranes. Descriptions of transducer electronics and other geotechnical instrumentation useful to hydrogeological studies can be found in Dunnicliff (1988).

17.4.5 Single-Well Hydraulic Tests

17.4.5.1 Constant-Head Injection Tests (CHITs)

Because open fractures may intersect a borehole at any depth, a continuous measurement of permeability with depth is necessary to locate these features. The most widely used method for testing individual boreholes is the constant-head injection technique. The principle behind a constant-head injection test (CHIT) is to inject or withdraw water at a constant hydraulic head into an isolated portion of the borehole

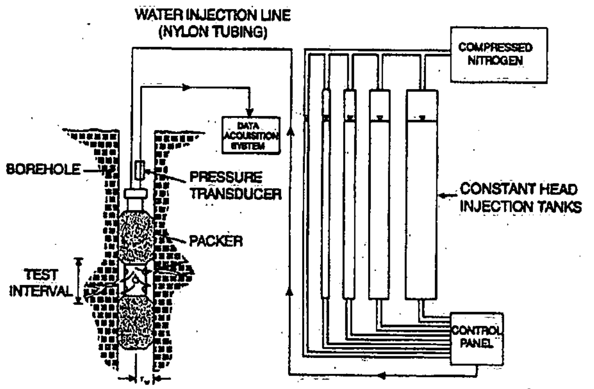

FIGURE 17.10 Schematic diagram of a typical constant-head injection testing system. A series of five tanks is shown on the right while the left shows the downhole instrumentation consisting of a two packer system and pressure transducer.

and measure the flow rate at steady-state conditions (Ziegler, 1976). CHITs may also be referred to as "Lugeon tests," or "constant pressure tests." While a pump and water supply could be used to inject water into the test zone, a series of different diameter tanks fitted with manometers is more commonly used and extends the limits of the testing apparatus to generate a wide range of injection flow rates (Figure 17.10). A range of 10^{-10} to 10^{-3} m²/s in transmissivity, *T*, can typically be determined using a series of three or more tanks ranging in diameter from 0.01 to 0.3 m. Flow rate is measured by timing the change in water level as viewed through the tank manometers. Compressed nitrogen gas added above the water in each tank ensures a constant flow rate as the tank empties. Flow meters can be used to measure flow rate; however, most flow meters have a very limited measurement range and thus a complex series of flow meters connected by valves would be required to achieve a range in measurement of *T* similar to the tank system.

Using measurements of flow rate, *Q*, and the change in pressure expressed as a change in hydraulic head, ΔH, at steady conditions, the *T* of the tested zone is calculated using the Theim equation:

$$T = \frac{Q}{\Delta H 2\pi} \cdot \ln\left(\frac{r_e}{r_w}\right) \tag{19}$$

The radius of influence, r_e, or outer flow boundary, can generally be assumed to be between 10 and 15 m for moderate values of *T* (Bliss and Rushton, 1984). While the actual radius of influence is unknown in most field situations, because it appears as a logarithmic term in Equation (19), large errors in estimation of r_e will result in only small errors in the calculation of *T*. Further discussion of this issue can be found in Doe and Remer (1980).

An equivalent single fracture aperture, $2b_{eq}$, can be determined from the test results by using the cubic law:

$$2b_{eq} = \left(T \cdot \frac{12\mu}{\rho g}\right)^{\frac{1}{3}} \tag{20}$$

The vertical distribution of *T* or $2b_{eq}$ is determined by systematically testing the length of the borehole in sections using a two-packer system. If possible, two to three increasing increments of pressure should be used during each test. In most studies, injection pressures leading to $\Delta H \leq 10$ m are recommended. Care must be taken not to use pressures that generate fracture dilation or hydro-fracturing. Figure 17.11

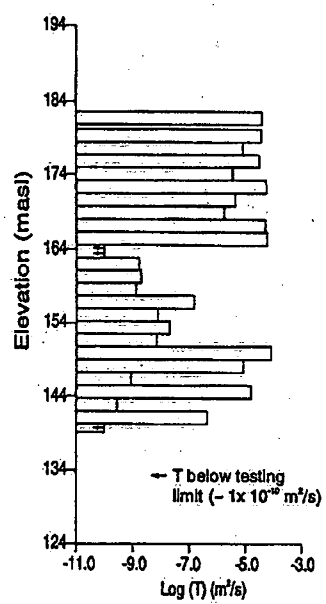

FIGURE 17.11 Typical profile of T with respect to depth obtained from a borehole drilled in Silurian dolostone and tested with constant-head injection tests using a 2-m packer test interval.

shows a typical profile of T with respect to depth obtained from a borehole drilled in Silurian dolostone. T varies by over seven orders of magnitude over 50 m illustrating the hetereogeneity commonly observed in fractured rock.

It is important to note that a single permeable fracture within a test zone will predominate the permeability measurement. Thus, the choice of test zone length will depend on the expected fracture spacing with depth. A too-short test interval will lead to an unnecessarily large number of tests, while a too-long test interval will not capture any of the variability in T and will lead to general overestimates of the permeability of the rock mass. To properly characterize a borehole in detail, an initial survey using a large packer separation length will identify the more permeable zones, while a subsequent second survey using a shorter packer separation length can be used to characterize the properties of individual permeable features and fracture zones (Figure 17.12).

17.4.5.2 Slug Tests

The slug (pulse or bail) test is a transient single-well method that is also frequently used in hydrogeological studies of fractured rock to obtain estimates of the hydraulic properties of a given length of borehole. Type curves based on radial flow in a confined porous aquifer are usually employed to obtain estimates of T and S (Cooper et al., 1967). Although, in principle, this method should provide estimates of T that are more accurate than CHITs, slug tests conducted in fractured rock frequently exhibit results which deviate from the ideal "Cooper et al., 1967" response. This has led to the development of numerous conceptual models which consider the effects of alternate boundary geometries, composite zones, and the other physical conditions more typically found in fractured rock systems. For example, in the presence of a damaged zone around the well, known as wellbore skin, T and S determined from a slug test may reflect only the skin zone (e.g., Faust and Mercer, 1984; Sageev, 1986). Wellbore skin can refer to a zone of enhanced permeability (negative skin) or of reduced permeability (positive skin). Double porosity effects (e.g., Doughtery and Babu, 1984), where both the fractures and matrix contribute to the flow system, can also be incorporated. Composite models are used to account for separate regions surrounding the well which have properties that are different from the formation properties as a whole (e.g., Moench and Hsieh, 1985; Karasaki et al., 1988). Open-hole slug tests are generally limited to zones of $T \geq 10^{-8}$

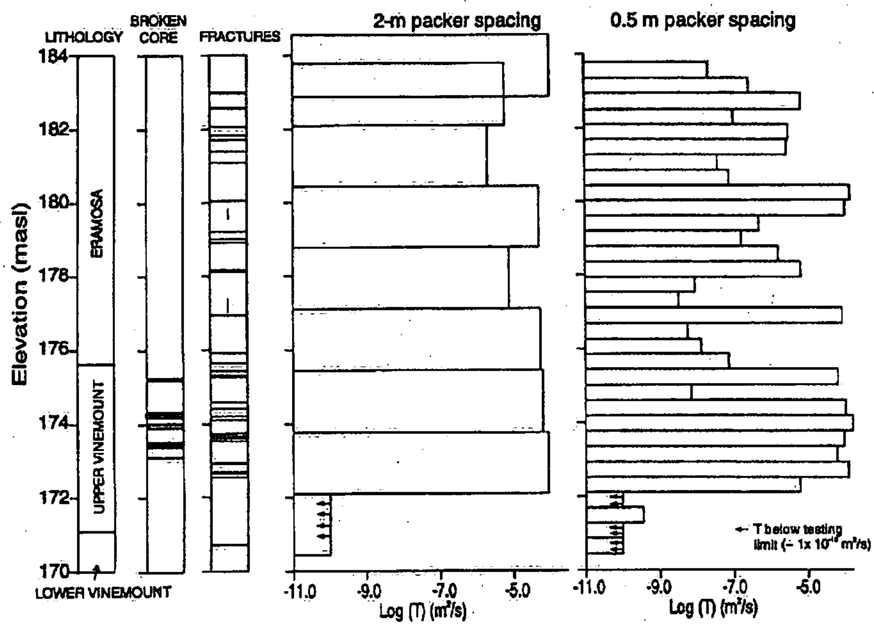

FIGURE 17.12 Results of two testing surveys (2-m and 0.5-m packer intervals) compared to fractures and broken core zones identified by core examination.

m^2/s due to the time required to achieve sufficient recovery for interpretation. In lower-permeability material ($T < 10^{-10}$ m^2/s) slug tests are conducted under shut-in conditions, reducing the effects of storage in the borehole (Bredehoeft and Papadopolus, 1980; Neuzil, 1982).

17.4.6 Multiwell Hydraulic Tests

17.4.6.1 Interference tests

In the following, the term "interference testing" is used to refer to all types of multiwell hydraulic tests. Interference testing between specific zones in two or more boreholes serves two main objectives: (1) establish the presence of hydraulic connection between the zones and (2) obtain estimates of interwell T and S. In the case of isolated discrete fractures, interwell aperture can also be calculated. In hydrogeological investigations, the choice of interference test method will be influenced by the diameter of the borehole, ability or desire to pump or inject large quantities of water into the formation, and the presence of a water table. Pumping tests conducted in fractured rock are done in a similar manner to those conducted in porous media. The difference lies in the factors influencing the response to pumping. Similar to the case for slug tests, pumping interference tests are influenced by: (1) wellbore storage, (2) skin effects, (3) double porosity, (4) boundary effects (e.g., a linear feature), and (5) vertical or subvertical fractures. Interpretation of interference tests is accomplished by matching the pressure or hydraulic head response in both the source and observation zones to theoretically derived response curves. This is accomplished by either manually matching field data to generated theoretical type curves (e.g., Earlougher, 1977) or using automated algorithms (e.g., Piggott et al., 1996).

17.4.6.2 Wellbore Storage

Fracture apertures usually range from a few microns to a few millimeters. Consequently, the volume of water stored in an open borehole will be several orders of magnitude greater than the volume of water in the fractures intersecting the borehole. This will influence the pressure response measured in the well during pulse interference and pumping tests. The wellbore storage factor, C_s, for an open well, is defined as πr_c^2 where r_c is the radius of the casing. The dimensionless wellbore storage coefficient, C_D, is defined as:

$$C_D = \frac{C_s}{2\pi r_w S} \tag{21}$$

where S is storativity of the rock formation. In low storativity media (most fractured rock systems), wellbore storage will significantly influence the early time response to a pressure disturbance in either a source or observation well. To accurately measure the hydraulic properties of low storativity media, wellbore storage must either be eliminated or accounted for in the interpretation of transient multiwell tests.

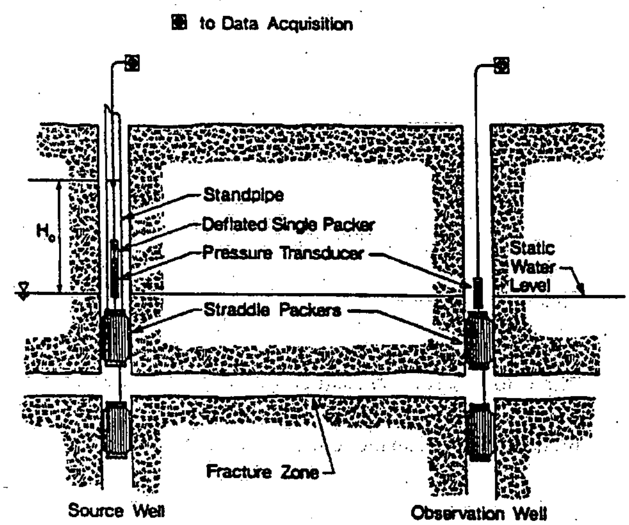

FIGURE 17.13 Schematic diagram showing field set-up for pulse interference tests. (From Novakowski, K. S. 1989. Analysis of pulse interference tests. *Water Resour. Res.* 25(11):2377-2387. With permission.)

17.4.6.3 Pulse Interference Tests

Single-pulse interference tests are an easy yet powerful extension to single-well slug tests. In this case, the pressure response in one or more observation zones due to the introduction of an instantaneous slug of water in a nearby source well is measured (Figure 17.13). A pulse interference test can be analyzed quickly using a graphical method (Novakowski, 1989). To do so, the magnitude of peak response and time lag in the observation zone must be measured. Peak response is defined as the ratio of the maximum rise in hydraulic head at the observation well (Δh) divided by the initial rise in hydraulic head in the source well (H_o). Time lag (t_L) is the elapsed time between the start of the slug test in the source well and the maximum peak response in the observation well. The remaining required dimensionless parameters (r_D, t_D), and dimensionless wellbore storage coefficients in both the observation and source well (C_{DO}, C_{DS}) are defined as follows:

$$r_D = \frac{r}{r_w} \qquad C_{DS} = \frac{C_s}{2\pi r_w^2 S} \qquad C_{DO} = \frac{C_o}{2\pi r_w^2 S} \qquad t_D = \frac{Tt_L}{r_w^2 S} \qquad \Delta h_{DO} = \frac{\Delta h}{H_o} \tag{22}$$

where r is the distance between the source and observation boreholes, and C_s and C_o are the storage coefficients in the source and observation boreholes, respectively. One of two sets of graphs is used to determine T and S using the dimensionless variables. Set 1 (Figure 17.14) is used when there is no observation well storage ($C_{DO} = 0$), whereas Set 2 (Figure 17.15) is used when the storage capacity in the source well is equal to the storage capacity in the observation well ($C_{DO} = C_{DS}$). First, using h_{DO} and r_D, a value for C_{DS} is determined from the graphs in part a, and S is calculated from the definition of C_{DS} in Equation (22). Second, using h_{DO} and r_D, a value for t_D is determined from the graphs in part *b*, and T is calculated from the definition of t_D in Equation (22). Figure 17.16 shows an example of both source and observation zone responses to a typical pulse interference test where $r = 22$ m, $T = 5 \times 10^{-4}$ m²/s, and $S = 4 \times 10^{-5}$.

17.4.7 Point Dilution Method

Measuring groundwater velocity in discrete fractures is often difficult because of the uncertainty associated with estimates of low hydraulic gradient (i.e., hydraulic head may vary by only centimeters over distances of many meters). The point dilution method may be employed to determine direct measurements of groundwater velocity. This method is based on the decay in concentration with time of a mixed tracer in a single well due to dilution caused by the natural groundwater flow through the borehole (Drost et al., 1968; Grisak et al., 1977). To conduct a point dilution experiment, a small section of the borehole having one or more fractures is isolated using a set of two pneumatic packers. To minimize the duration of the experiment, the mixing volume must be reduced by using a short spacing between the two packers. The experiment is initiated by instantaneous injection of a small volume of conservative tracer into the test zone, and mixing is continued throughout the duration of the experiment. Figure 17.17 shows schematically a typical arrangement for a point dilution experiment. Suitable conservative tracers include bromide or chloride, some fluorescent dyes (e.g., Lissamine FF), radioactive isotopes (e.g., tritium), or stable isotopes (e.g., deuterium).

The decay in concentration is interpreted using (Drost et al., 1968):

$$\frac{dc}{dt} = -Av_a \frac{c}{V} \tag{23}$$

where A is the cross sectional area available to flow, v_a is the apparent velocity of groundwater flowing through the wellbore, and V is the volume of the sealed-off portion of the borehole in which the dilution occurs. The solution to Equation (23) for the case of instantaneous injection and relating the apparent velocity in the test section to the true formation velocity, v_f, yields (Drost et al., 1968):

$$v_f = \frac{V}{\xi A t} \ln \frac{c}{c_o} \tag{24}$$

where c_o is the initial concentration at $t = 0$, c is the concentration at time t after the tracer was injected, and ξ is a dimensionless correction factor accounting for additional flow captured by the open well due to the convergence of flow lines in the neighborhood of the wellbore. Groundwater velocity in a single fracture intersecting the test zone (v_f) is determined from the measurements of dilution of tracer in the sealed off portion of the borehole by plotting the results in the form of ln c vs. t and fitting a linear regression line to the data (Figure 17.18). Using the time (t_m) at $c/c_o = 0.5$ from the regression line, Equation (24) reduces to:

$$v_f = \frac{0.693V}{\xi A t_m} \tag{25}$$

(a)

(b)

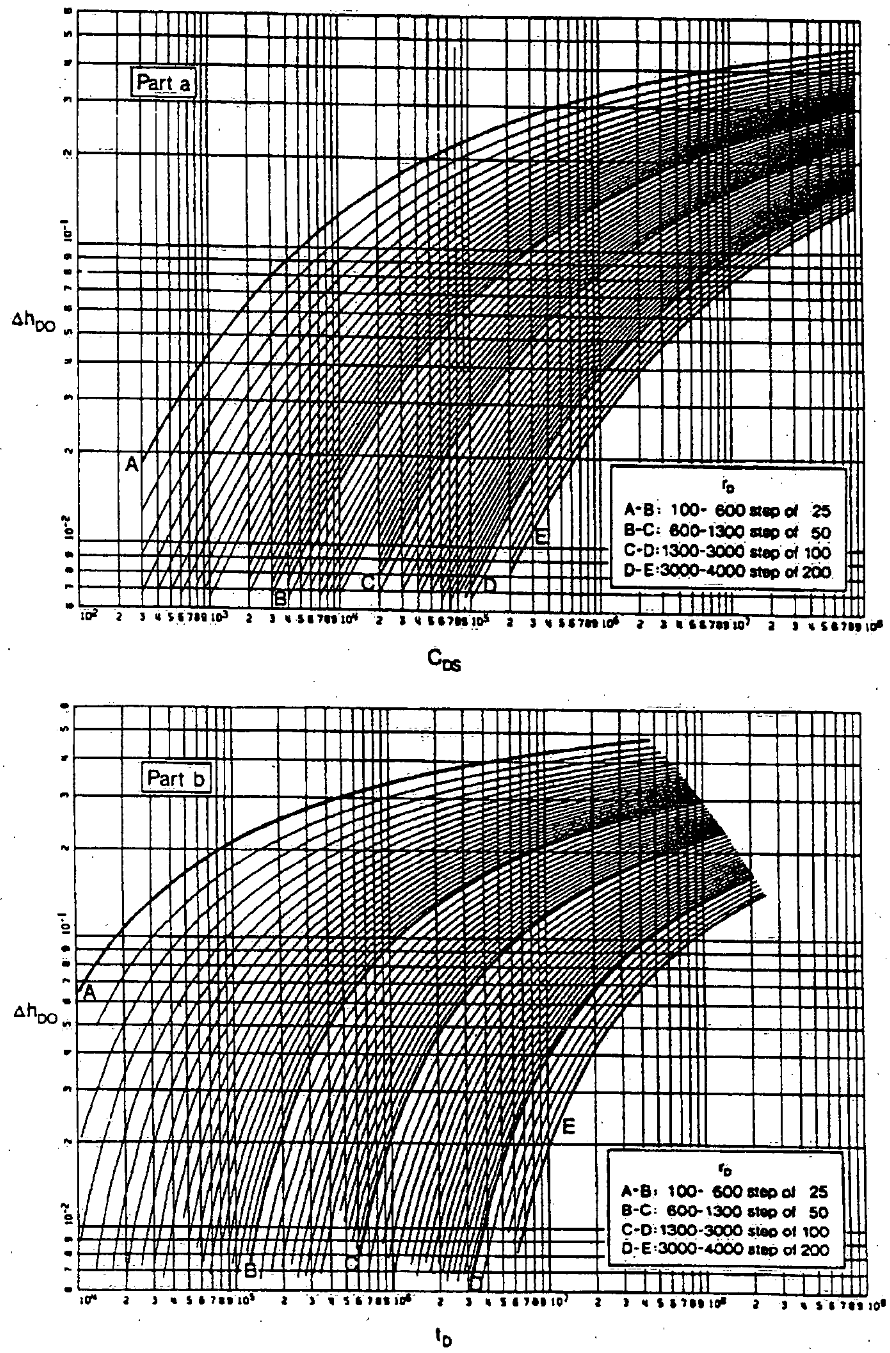

FIGURE 17.14 Type curves used to interpret pulse interference tests by graphical method when there is no observation well storage (a) curves used to calculate S and (b) curves used to calculate T. (From Novakowski, K. S. 1989. Analysis of pulse interference tests. *Water Resour. Res.* 25(11):2377-2387. With permission.)

(a)

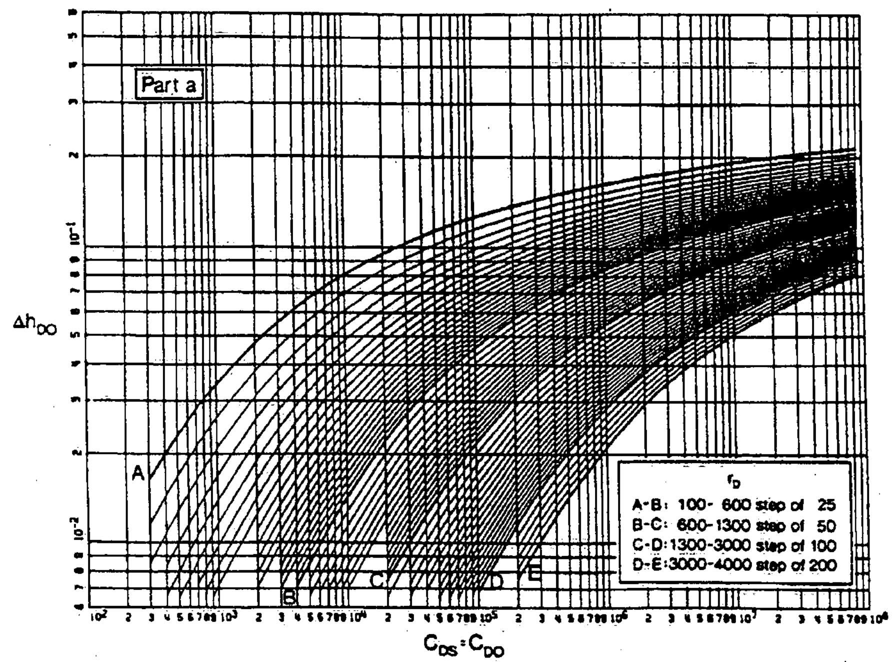

(b)

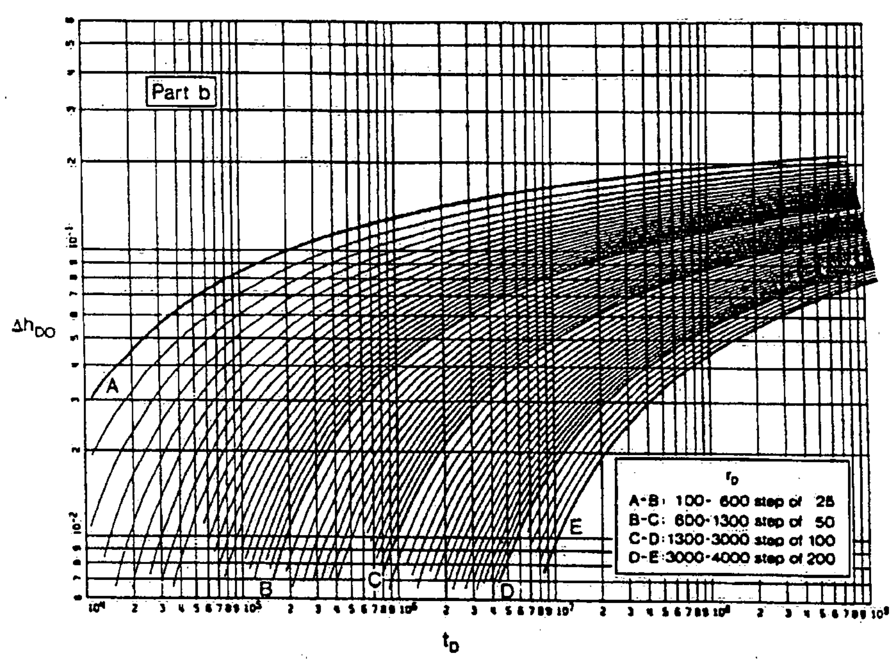

FIGURE 17.15 Type curves used to interpret pulse interference tests by graphical method when observation well storage = source well storage (a) curves used to calculate S and (b) curves used to calculate T. (From Novakowski, K. S. 1989. Analysis of pulse interference tests. *Water Resour. Res.* 25(11):2377-2387. With permission.)

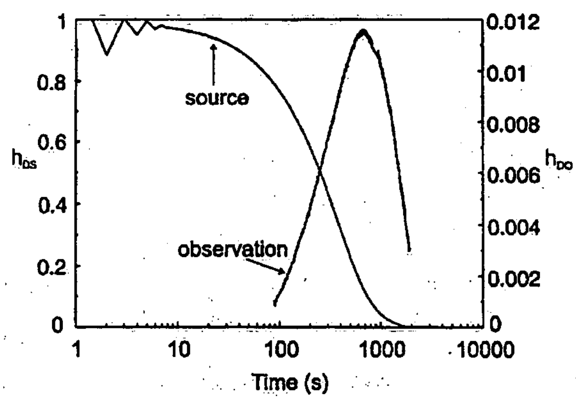

FIGURE 17.16 Example of source well pulse and observation zone response. Test was conducted in a 500-μm fracture where the observation zone was approximately 22 m from the source zone.

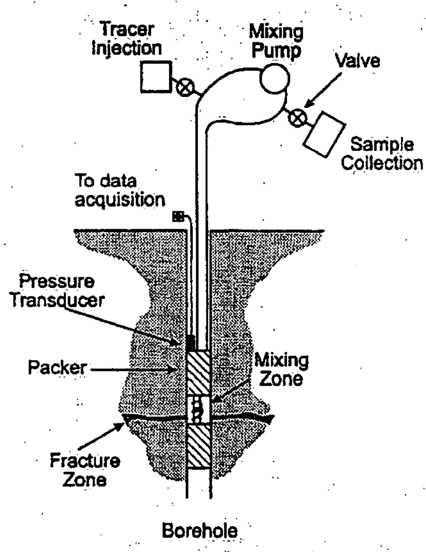

FIGURE 17.17 Schematic diagram of the experimental apparatus used for a point dilution.

In the case of a zone containing a single fracture, $A = 1/2$ the circumference of the borehole times the hydraulic aperture and $\xi = 2$. Where more than one fracture intersects the borehole, the interpretation is more complicated. To accurately estimate velocity, the aperture of each individual fracture should be known, otherwise the result will represent an average.

17.4.8 Tracer Experiments

Tracer experiments conducted in fractured rock provide a means of determining solute transport parameters (i.e., velocity, dispersivity, and matrix porosity) of individual fractures or fracture zones at the field scale. Similar to tests in porous aquifers, tracer experiments conducted in fractures can be carried out using either forced hydraulic gradient or natural gradient flow conditions. Because of the difficulty and cost associated with natural gradient tracer experiments, very few of these have been conducted and no further discussion of this method will be presented here. In the following, the common methodologies used to carry out multiwell tracer experiments under conditions of forced gradient are outlined.

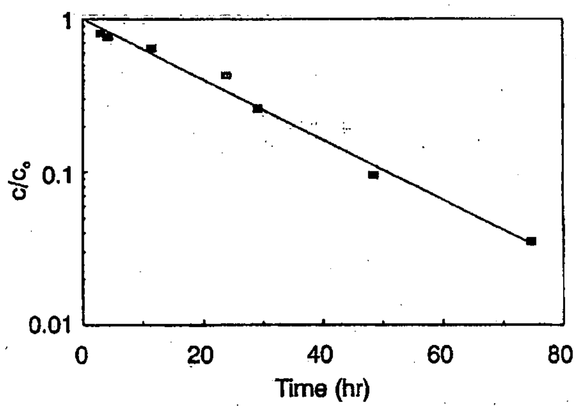

FIGURE 17.18 Example point dilution response curve. In this test a velocity of 4 m/day was measured in a 220-μm fracture.

The three flow field geometries which are commonly used when conducting tracer experiments under forced gradient in fractured rock are: (1) injection-withdrawal, (2) radial convergent, and (3) radial divergent. In the injection-withdrawal format, an artificial steady-state flow field between two wells is established where the injection flow rate is equal to the withdrawal flow rate (Figure 17.19a). Tracer is introduced either as a finite slug or continuously into the injection well, and the concentration is monitored at the withdrawal well. An example of this type of experiment can be found in Novakowski et al. (1985). The water removed from the withdrawal well can be re-circulated back into the system via the injection well, but this will complicate the interpretation of the test. The advantage to this test method is the development of a well controlled flow field where recovery of the tracer should approach 100%. A radial-convergent experiment is conducted by passively injecting tracer into one borehole and withdrawing by pumping at a second borehole (Figure 17.19b). Multiple source boreholes can be used by introducing a different tracer in each. An example of the use of this experimental method is outlined in Shapiro and Nicholas (1989). Radial-divergent experiments are conducted by injection of tracer in a single well and passively monitoring the tracer arrival in one or more observation wells (Figure 17.19c). An example of this experiment is presented in Novakowski and Lapcevic (1994). The choice of methodology will depend on the objectives of the experiment, the number of boreholes available for study, the ease of pumping and sampling, and the type of tracer used.

To date, most forced-gradient experiments have been conducted in discrete fractures or fracture sets in which the geometry of the fracture is well known (e.g., Raven et al., 1988; Shapiro and Nicholas, 1989; Abelin et al., 1991). The scale of these experiments has been limited to interwell travel distances of 50 m or less. In future, tracer experiment methodology should prove very useful in confirming the geometry of fracture intersections, the presence of which may be surmised from the results of interwell hydraulic tests. Interwell distances for tracer experiments will likely increase.

17.4.9 Borehole Instrumentation

Permanent completion of boreholes drilled in bedrock is generally carried out in one of two ways: (1) using technology designed for piezometer construction in unconsolidated porous media or (2) through the use of multilevel borehole casing. Only the latter will be discussed in this chapter; the former is covered in discussions of well completions for unconsolidated porous media. Multilevel completions are primarily designed to: (1) obtain measurements of hydraulic head and (2) obtain representative samples of groundwater. This is accomplished by isolating sections of the borehole using a series of permanent packers joined by casing or riser pipe. Access to the isolated zones is through manometers or access ports. Currently, two commercial systems of multilevel completions are widely used around

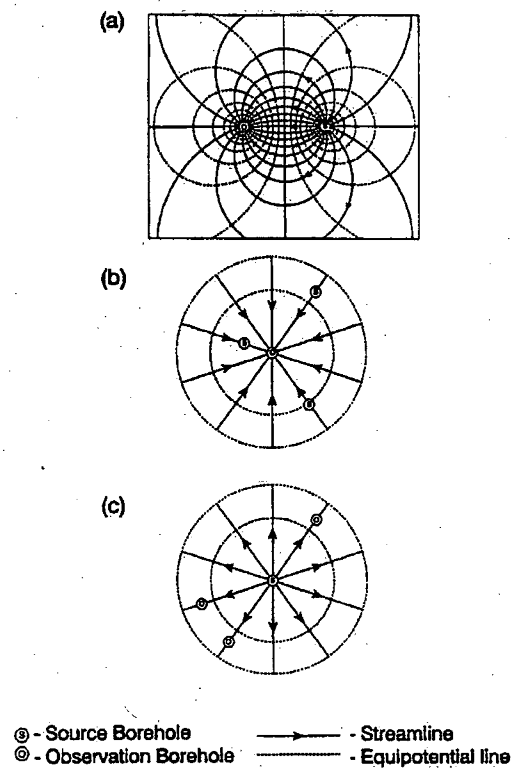

FIGURE 17.19 Flow field geometry commonly used for tracer experiments: (a) injection-withdrawal, (b) radial convergent, and (c) radial divergent.

the world. These are the Solinst® system (Cherry and Johnson, 1982) and the Westbay® system (Black et al., 1987). The advantage to multilevel casing is that numerous distinct zones may be accessed in a single borehole.

The Solinst system (Figure 17.20) is based on packers that are filled with a sealant chemical that is activated by the introduction of water into the casing after the complete casing string has been lowered into the borehole. Sampling ports and manometers of thin nylon or Teflon® tubing provide access to each sealed-off zone to measure water levels and withdraw groundwater samples. Triple-tube sampling pumps can either be installed in each zone or lowered into the manometers. These pumps allow sampling in zones where pumping from the surface is not feasible. Additionally, pressure transducers or transmitters can be included in each zone to electronically measure water pressure. Depending on the objectives of the study and specific site conditions, the modular instrumentation system can be customized to maximize the amount of data obtained. The number of zones sampled or measured is limited by the diameter of the borehole (and thus the diameter of the casing) as each transducer, pump, or sampling port requires access to the surface through tubing or electrical cable.

The Westbay system is also a modular design having water-filled packers connected by casing elements and specially designed pumping and measurement/sampling ports (Figure 17.21). Water pressure is measured and representative groundwater samples are obtained using a submersible probe which is lowered into the casing and connected to an electronic data acquisition device on the surface. The probe has a small arm which is used to locate each measurement port inside the casing. Once positioned on the port, a mechanical foot on one side of the probe is activated and presses against the inner casing wall. This causes an o-ring on the opposite side of the probe to seal around a ball bearing and exposes the pressure transducer in the probe to water pressure outside the casing. Groundwater samples can be

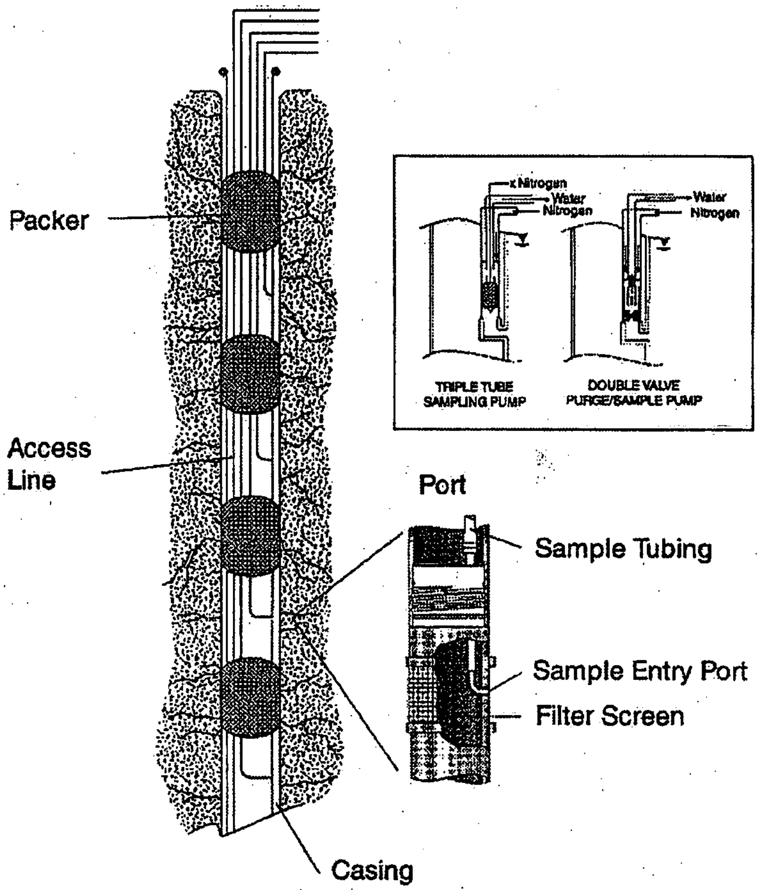

FIGURE 17.20 Components of the Solinst® system of permanent multilevel instrumentation for use in the rock boreholes. Access lines may be electrical cables for pressure transducers installed in the ports or tubing to sample the isolated zones. Pumps (triple tube or double valve types) may be dedicated to specific zones or lowered into the sampling tubing as required. Manual water level measurements are obtained through the tubing.

obtained using the same port by opening a valve from the surface unit and allowing water to fill a sample container attached below the probe (Figure 17.21).

Additionally, in some instances, hydraulic tests can be conducted after permanent multilevel completions have been installed. For example, a borehole instrumented with several zones, used as an observation well during a pumping test can provide information on the vertical connection of fracture zones. To maximize the data obtained from permanently instrumented boreholes, care must be taken in designing appropriate isolated zones. Careful examination of rock core, geophysical surveys, and hydraulic testing results prior to installation of the instrumentation will ensure that the isolated zones appropriately define the three-dimensional nature of the groundwater flow system.

17.5 Conceptual Models

In formulating an understanding of groundwater flow and solute transport for a given site or region at which flow is dominated by the presence of fractures, it is important to develop a reasonable conceptual model as a starting point. In many cases, the conceptual model may incorporate elements of the flow system at a variety of scales. This may include processes at the microscopic scale, such as matrix diffusion,

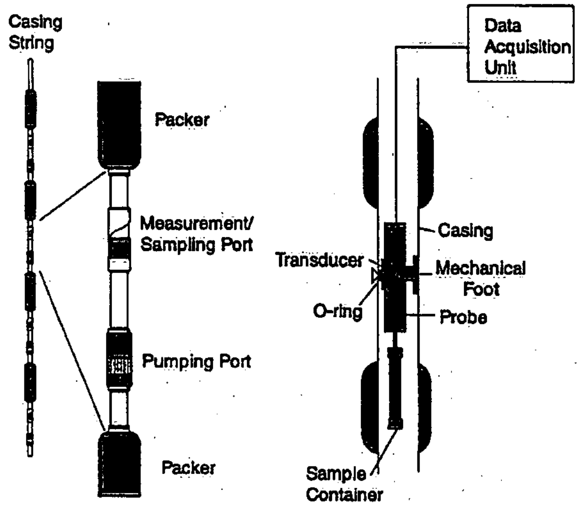

FIGURE 17.21 Components of the Westbay® system of permanent multilevel instrumentation for use in the rock boreholes. Note that no tubing or electrical cable is permanently installed in the casing string since the probe is lowered to each zone to either measure water pressure or obtain a groundwater sample.

and processes at the single-continuum scale, such as recharge or discharge. In the following section, a variety of conceptual models for flow and transport at the scale of a discrete fracture and a fracture network are discussed. In all cases, it is assumed that the cubic law, hydrodynamic dispersion, and matrix diffusion apply at the microscopic scale.

Bear (1993) defined four operational scales in a fractured medium, at which different conceptual approaches might be applied (Figure 17.22). At the very-near field scale, flow and solute transport are dominated by a single fracture. At the near field, flow and transport are dominated by a few well-defined fractures, and interaction between the fractures and the matrix may play a role. At this scale, discrete fracture models may be used in which the major fractures are defined deterministically and the minor fractures are specified stochastically. Depending on the type of fractured rock, it is likely the near-field scale that is of most interest to practicing hydrogeologists. At the far-field scale, multiple continua are defined using at least one continuum for the unfractured matrix, possibly one for the minor fractures and another for the major fractures. At the very-far-field scale, a single continuum can be applied. In particular cases, it may be found that a mixture of conceptual approaches is required. For example, in some sedimentary rock environments, sheeting fractures may predominate in one stratigraphic horizon, while in another the fracturing is so frequent as to warrant the use of a continuum or a multicontinuum approach.

17.5.1 Conceptual Models for a Single Fracture

Numerous studies have been conducted in which the roughness of natural fracture walls and the distribution of fracture aperture have been measured (e.g., Brown et al., 1986; Gentier and Billaux, 1989; Piggott, 1990). These studies have been conducted on fracture samples ranging in scale between 0.1 and 1 m. The results indicate that the surfaces of fracture walls can be rough and undulating with numerous contact points between the walls. In general, it is concluded that (1) fracture aperture may fit into one of several statistical distributions, (2) aperture is correlated spatially, and (3) aperture distributions are scale invariant.

The distribution of apertures at the laboratory scale has been observed to follow either a log-normal distribution (Gentier and Billaux, 1989; Hakami, 1995), a Gaussian distribution (Piggott, 1990; Brown, 1995; Hakami, 1995), or a gamma distribution (Tsang, 1984). Additionally, spatial distributions of

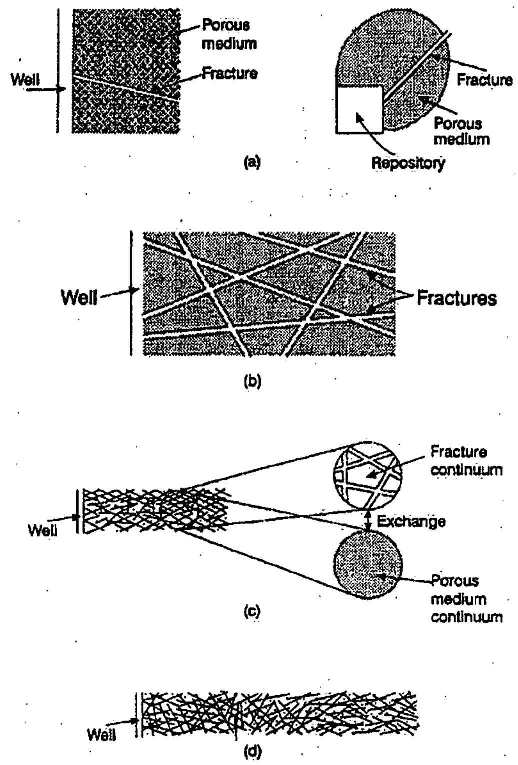

FIGURE 17.22 Operational scales in a fractured medium: (a) very-near field, (b) near field, (c) far field, and (d) very-far field. (From Bear, J. 1993. Modeling flow and contaminant transport in fractured rocks, in *Flow and Contaminant Transport in Fractured Rocks.* Eds. J. Bear, C.-F. Tsang, and G. de Marsily. Academic Press, San Diego, 1-37. With permission.)

aperture are often observed to have a large variance, indicating a high level of heterogeneity in the fracture plane (e.g., Hakami, 1995). The roughness of fracture surfaces has also been determined to display fractal properties implying that variable aperture distributions may be scale invariant (e.g., Brown et al., 1986; Wang et al., 1988).

Fractures with similar statistical distributions of aperture may have very different flow properties due to the spatial relation of the aperture variations. Fracture surfaces have been determined to be correlated spatially with the degree of correlation related to the scale of measurement. Brown et al. (1986) determined correlation lengths from between 0.5 and 5.0 mm for sample lengths and diameters of 25.4 mm. Vickers et al. (1992) studied surface roughness of a single fracture in a block of welded tuff (0.15×0.40 m) and found the resulting aperture distributions close to normal except at the tails. The apertures were also found to be correlated at two scales, one on the order of millimeters and the other on the order of tens of centimeters. In addition, Vickers et al. (1992) found that apertures increased consistently along the entire length of the fracture, suggesting that a third spatial correlation occurs at a scale well in excess of the sample dimensions. Hakami (1995) compiled experimental results of aperture measurements at the lab scale and concluded that both the variance and spatial correlation length increase with increasing mean aperture.

It is also well recognized that the regions in which the fracture surfaces are in contact and closed to water flow will strongly influence flow and transport. Experiments conducted by injecting wood's metal into fractures in granitic cores have shown contact areas ranging from 8 to 15% with a normal stress of 3 Mpa (Pyrak-Nolte et al., 1987). At the field scale, hydraulic aperture measurements in two fractures at depths less than 15 m in sedimentary rock (shale/limestone) in an area roughly 30 m × 30 m, indicate fracture closure between 20 and 30% (Lapcevic et al., 1990). Smooth fractures will display many small areas of contact with complex outlines resulting in a complex distribution of fluid flow among many small channels. In contrast, rough fractures display fewer, larger contact areas with smoother outlines concentrating flow in a few large channels (Odling, 1994). Tsang (1984) observed that increases in contact area results in a reduction in mean aperture, an increase in tortuosity, and a decrease in the connectivity of the fluid flow paths. Tortuosity factors determined through comparisons of measured hydraulic versus physical apertures have been observed to be a good approximation to account for closure (e.g., Piggott and Elsworth, 1993).

Experimental studies of flow and transport in laboratory-scale fractures have been used to investigate the relationship between measured apertures and resultant flow characteristics within the fracture. Results of flow experiments on fractures in laboratory studies with known aperture distribution show that the ratio between mean aperture and hydraulic aperture is 1.1 to 1.7, for $0.1 < 2b < 0.5$ mm (Hakami, 1995). The lower value of the hydraulic aperture is to be expected since the variation in aperture of natural fractures forces the flow to be tortuous. It is well recognized that fluid flow in natural fractures will be controlled by the distribution of asperities leading to tortuous paths and areas in which no flow occurs.

There are several conceptual models for transport in a fracture of variable aperture. For example, the "channel model" for flow and transport through a single fracture is based on a series of one-dimensional channels of constant aperture oriented in the direction of flow (Tsang and Witherspoon, 1983). Tsang and Tsang (1987) extended this model to include a limited number of tortuous and intersecting channels each characterized by an aperture density distribution, effective channel width, and correlated in length and aperture (Figure 17.23). A gamma function was used to characterize the aperture distribution and standard geostatistical techniques used to calculate distributions. Johns and Roberts (1991) presented a two-aperture channel model in which lateral transfer of mass from large to small aperture regions of the fracture plane and vertical diffusion into the rock matrix were considered. Moreno et al. (1988) presented a stochastic model in which flow and transport in the entire fracture plane were considered. The aperture of the fracture was lognormally distributed and possessed a spatial correlation length (λ). From this it was concluded that a broad distribution of apertures with spatial correlation length on the same order of magnitude as the scale of measurement is responsible for flow channeling phenomena.

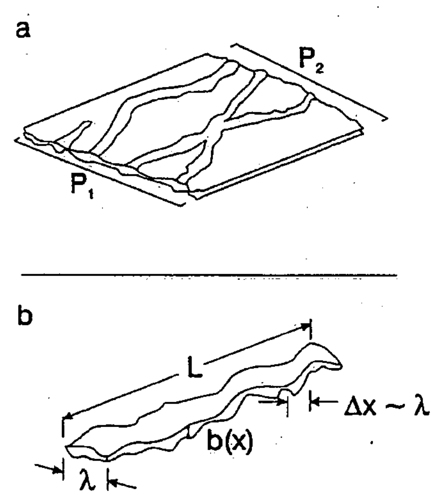

FIGURE 17.23 (a) Channel representation of fluid flow in a single fracture, and (b) schematic sketch of one channel, where b(x) is the aperture distribution, and λ is the spatial correlation length of the distribution. (From Tsang, Y. W. and Tsang, C. F. 1987. Channel model of flow through fractured media. *Water Resour. Res.* 23(3):467-479. With permission.)

Determining the spatial distribution and correlation of fracture aperture at the field scale is difficult because of the extreme cost required to obtain sufficient field data. Consequently, conceptual models of variable aperture based on surface roughness are well verified at scales up to a meter but have yet to be verified with field data at scales in the tens to hundreds of meters. Thus, we are left with using simple correction factors such as macroscopically defined tortuosity to account for this variability.

17.5.2 Conceptual Models for a Fracture Network

In all rock types, fractures of various sizes and lengths combine to form three-dimensional networks of interconnected groundwater pathways. At scales less than that defined for a single continuum, determining an appropriate conceptual model for the three-dimensional arrangement of fractures is essential in understanding and predicting groundwater flow and solute transport in fractured rock. In general, a distinction must be made between conceptual network models for sedimentary rock and those for crystalline rock. In most sedimentary rock environments, the directions of the principal fractures follow bedding planes and other pre-existing planes of weakness related to deposition. These fractures are often connected by near-orthogonal fractures whose genesis is related to paleo- and neotectonic stresses (Holst, 1982; Williams et al., 1985). For flat-lying stratigraphy, this results in a relatively simple fracture framework which can be conceptualized by several discrete horizontal fractures connected by statistically defined sets of subvertical fractures. Figure 17.24 illustrates a typical three-dimensional view of a conceptual fracture framework for a layer-cake stratigraphy. Note that the vertical fractures are constrained by the bedding and have a preferred orientation. There are exceptions to this scenario, however, for sedimentary environments which have undergone considerable deformation. In such cases, the stratigraphy tends to be inclined and folded. This concentrates vertical fractures in the vicinity of fold axes and leads to shearing movement on some bedding planes. Other salient features of the conceptual model for flat-lying stratigraphy are retained, however.

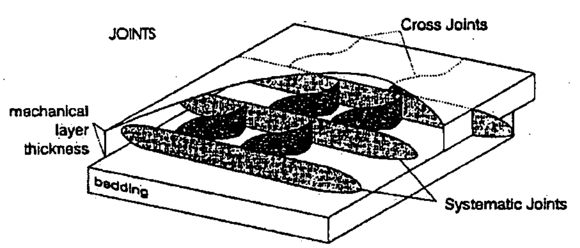

FIGURE 17.24 Typical three-dimensional view of conceptual fracture framework for a layer-cake stratigraphy. (From Engelder, T., Fischer, M. P. and Gross, M. R. 1993.*Geological Aspects of Fracture Mechanics, A Short Course Manual*, Geological Society of America, Boulder, CO. With permission.)

Conceptual models for crystalline rock environments are usually more complex than that for sedimentary rock. In uniform granitic rock, fractures may be oriented in preferred directions according to magma emplacement and cooling (polygonal fracture sets), local deformation, regional deformation, and erosional unloading (sheeting fractures).

One of the earliest conceptual models for flow in crystalline rock was based on the assumption of an equivalent porous medium (Snow, 1969). The concept was developed to relate the results of permeability measurements obtained from boreholes to a hydraulic conductivity ellipsoid which defines the anisotropic permeability of the bulk rock. To conduct the interpretation, it was assumed that flow was predominated by the fractures, all fractures contributed to the flow system, and the orientation of the fractures intersecting the boreholes was known. The hydraulic conductivity ellipsoid was constructed by summing the permeability contributions of each fracture intersecting each test interval.

It has long been recognized that fractures form disc-shaped discontinuities, particularly in granitic environments. Figure 17.25 shows a three-dimensional conceptual model in which disc-shaped fractures

FIGURE 17.25 Three-dimensional conceptual model of disc-shaped fractures which are of random size and oriented orthogonally. (From Long, J. C. S., Gilmour, P., and Witherspoon, P. A. 1985. A model for steady fluid flow in random three-dimensional networks of disc-shaped fractures. *Water Resour. Res.* 21(8):1105-1115. With permission.)

are of random size but oriented orthogonally. This concept can be extended to the general case for more random orientations of discs. For example, Cacas et al. (1990) and Dverstorp et al. (1992) have developed numerical flow and transport models based on a three-dimensional distribution of discs randomly placed in space and of random radius, but given a specific spatial orientation to simulate fracture sets. Groundwater flow and solute transport were then assumed to follow one of three types of linear flow channels which interconnect the individual fractures in the network (Figure 17.26).

Recently, scaling relations have been introduced into these types of conceptual models through the use of fractals, thus providing a method of using field data in the generation of artificial fracture networks. Figure 17.27 illustrates the generation of a three-dimensional network of fractures based on fracture traces measured from outcrop scan lines, air photographs, and geophysical data (Piggott et al., 1997). From the trace data (Figure 17.27a) statistically generated two-dimensional traces are extended to produce the three-dimensional network of fractures (Figure 17.27b). A detailed three-dimensional view of a portion of the fracture network in Figure 17.27b is shown in Figure 17.27c.

17.6 Modeling Flow and Transport in Fractures and Fracture Networks

In some cases, such as where sheeting fractures dominate the groundwater flow system, it may be necessary only to model these discrete features and not the flow system as a whole. Simple analytical models for flow and transport in a single fracture (e.g., Tang et al., 1981) or a set of parallel fractures (Sudicky and Frind, 1982) may suffice. For example, transport calculations such as those shown in Figure 17.7 may provide the information necessary to illustrate the potential importance of matrix diffusion at a given site.

Nonconstant aperture in the fracture plane, as discussed in the previous section, will influence solute transport in single fractures. Direct solution of the flow and transport in a fully defined aperture distribution can be conducted using numerical models (e.g., Lapcevic, 1997). For example, Figure 17.28 compares a tracer plume created assuming a constant aperture to one simulated assuming a spatially variable aperture. Note that the variability in aperture leads to a plume of much greater irregularity in

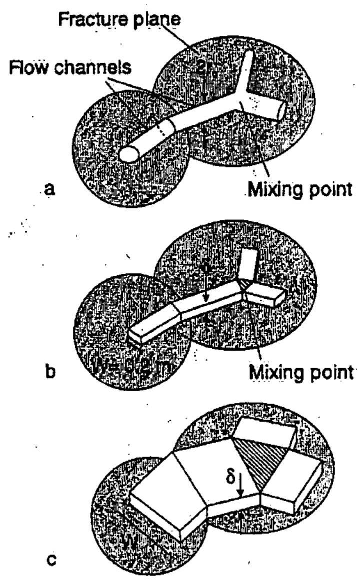

FIGURE 17.26 Three types of interconnecting flow channels in a fracture network: (a) tubular flow channels, (b) parallel plate channels with constant width, and (c) parallel plate channels with width equal to the fracture intersection line. (From Dverstorp, B., Andersson, J., and Nordqvist, W. 1992. Discrete fracture network interpretation of field tracer migration in sparsely fractured rock. *Water Resour. Res.* 28(9):2327-2343. With permission.)

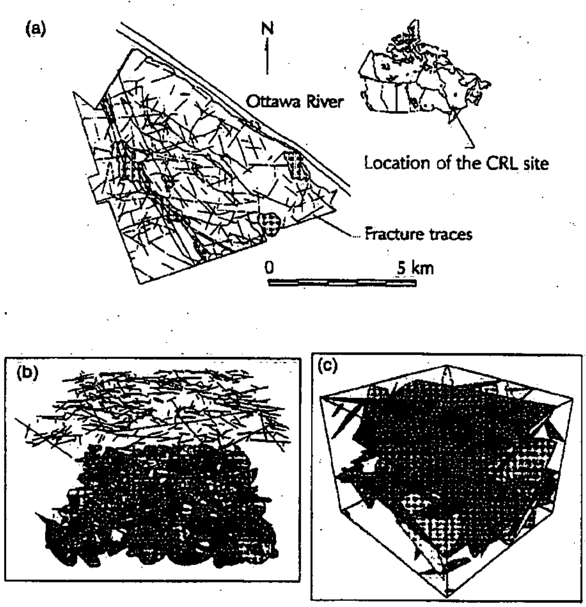

FIGURE 17.27 Generation of a conceptual model of fracture network using field data and fractal relations: (a) fracture traces measured from outcrop scan lines, air photographs, and geophysical surveys, (b) statistically generated two-dimensional traces (top) extended to form three-dimensional network of fractures (bottom), and (c) detailed portion of network shown in bottom part of (b). (From Piggott, A., Moltyaner, G., Yamazaki, L., and Novakowski, K. 1997. Preliminary characterization of fracturing at the site of the Chalk River Laboratories, in *Proceedings of 50th Canadian Geotechnical Conference*, Ottawa, Canada (also NWRI No. 97-126). With permission.)

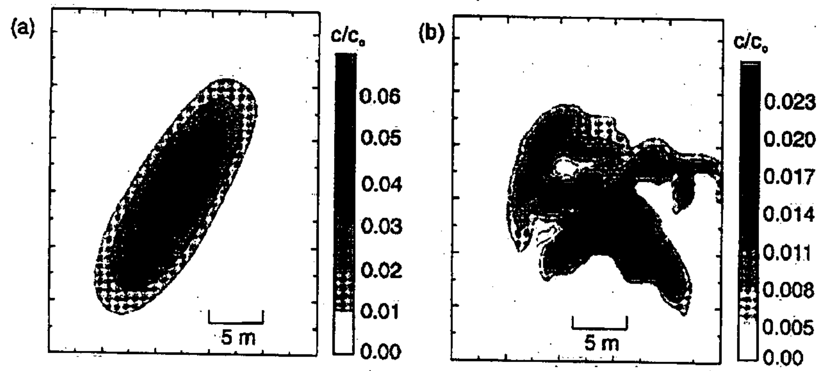

FIGURE 17.28 Two-dimensional concentration plumes in a single fracture illustrating the effect of variable aperture on plume dimensions: (a) tracer plume assuming a constant aperture, and (b) tracer plume assuming aperture of the fracture is variable.

shape and of lower peak concentration. Thus for some distributions of aperture it may be necessary to consider variable aperture in simulation at the discrete fracture scale. Unfortunately, in almost all field studies there is insufficient information to generate a defensible model of variable aperture.

Modeling approaches to simulate flow and transport in fracture networks fall into one of three categories within the range of conceptual models for fractured rock: (1) equivalent porous medium (EPM), (2) dual porosity, (3) discrete fracture representation. In addition, fracture network models may be implemented in either two or three dimensions.

Models based on equivalent porous medium treat the fractured porous rock as equivalent to a non-fractured continuum. Bulk parameters for the permeability of the rock mass are used, and the geometry of individual fractures or the rock matrix is not considered. This is a reasonable approach if fracturing is intense or the study domain is sufficiently large such that individual fractures have no influence on the overall flow system (e.g., some regional systems of the scale of kilometers). Berkowitz et al. (1988) and Schwartz and Smith (1988) discuss the use of continuum models for fractured rock systems.

Raven (1986) applied a continuum model using a detailed set of hydraulic testing results obtained from a small flow system in a monzonitic gneiss. Constant-head injection tests were conducted using contiguous test intervals in 17 boreholes of approximately 50-m depth. Using BHTV, fracture orientation and frequency was determined for each test interval. By assuming each fracture intersecting a given test interval was of equal aperture, the CHIT result was related to an effective permeability tensor for the interval (Snow's method described in the previous section). The tensor was diagonalized to determine the principal directions and principal values of the hydraulic conductivity ellipsoid. These values were then used in a two-dimensional finite-element model based on a single continuum to evaluate the degree to which the conceptual model (i.e., equivalent porous media) could predict the flow of groundwater through the rock mass. Results indicated that the conceptual model and numerical approach could adequately describe flow conditions in the shallow subsurface (<30 m), but could only poorly describe these at greater depths. This was attributed to the inadequacy of the conceptual model in incorporating vertical flow conditions which were more prevalent at depth in this site. It should also be noted that the conceptual model was not tested against the transport properties of the fracture system.

Double porosity models are used to attempt to bridge the gap between the simplifications of EPM models and the details of the discrete fracture models by treating the fracture system and the porous matrix as two separate inter-related continua (Barenblatt et al., 1960). In this approach, equations of flow and transport for each system are linked by a source/sink term that describes the fluid or solute exchange between the two systems each of which may have very different properties relative to the other. Examples of semianalytical and numerical models having this approach can be found in Huyakorn et al. (1983), Rowe and Booker (1990), and Sudicky (1990). Some limitations to the double porosity approach

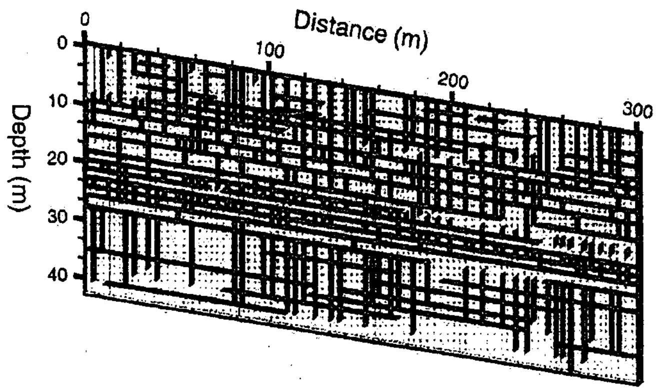

FIGURE 17.29 Network of orthogonal fractures generated based on a conceptual model of layered sedimentary rock where each layer has differing fracture spacing and connectivity parameters. System is divided into three layers: a densely fractured zone (0 to 26 m), a relatively unfractured zone (26 to 28 m), and a more sparsely fractured zone (28 to 45 m).

include the assumption that the matrix blocks are of simple (and possibly unrealistic) geometry and that advection of solutes in each block is ignored.

The discrete fracture approach will result in the most physically representative simulation of flow and transport processes at the subcontinuum scale. However, discrete fracture models require the generation of fracture networks based on a working conceptual model developed using information on both the individual fractures and the geometry of interfracture relationships. A network of fractures is characterized by a distribution of fractures of fixed or variable aperture, finite length, regular or random orientations, and some degree of connectivity with other individual fractures. Thus, the development of the conceptual model strongly influences the outcome of the model simulations. Figure 17.29 illustrates a fracture network generated using a conceptual model of fracturing in a layered sedimentary sequence of dolostone and shale. To generate this network minimum horizontal and vertical fracture spacings of 1.5 m and 3.5 m were set for the entire sequence. Within each geologic unit a range of fracture lengths and fracture density were set. Note the denser fracture zones at the top of the sequence (0 to 26 m), a relatively unfractured zone at 26 m, and a more sparsely fractured zone from 28 m to 45 m.

17.6.1 Flow in Discrete Fracture Networks

The modeling of flow in discrete fracture networks may be conducted to estimate groundwater flux for the purpose of groundwater resource evaluation or to provide an estimate of the distribution of groundwater velocity in individual fractures as input to a solute transport model. In the former case, transient hydraulic head conditions may be of interest, whereas in the latter, only steady conditions are considered. In the following, two approaches to the modeling of flow in discrete features are described. Both are suitable for either transient or steady flow conditions.

Barker (1991) developed a robust semianalytical method which can be used to determine the distribution of groundwater flux and velocity in a two-dimensional network of fractures having random orientations. The fracture network is conceptualized as a linked system of linear elements for both steady and transient flow conditions (e.g., Dverstorp et al., 1992). Flux into each node is calculated by summing the contribution from each fracture using Darcy's law. The cubic law is used to relate the fracture aperture to elemental hydraulic conductivities. The system of Laplace transformed equations is solved by direct or iterative methods depending on the size of the network and the results numerically inverted from the Laplace domain to obtain values in real space.

Modeling groundwater flow in three-dimensional fracture networks is considerably more difficult than for two-dimensional slices. For conceptual models involving sparsely distributed fractures in impermeable rock, randomly oriented fracture discs and fracture intersections of various orientations must be discretized. However, the mesh generation required for solution with standard finite element or finite difference techniques is prohibitively difficult, even for small solution domains. Alternative solution methods have been attempted including a hybrid analytical–numerical scheme (Long et al., 1985) and a boundary element formulation (Elsworth, 1986), but these were found not to be generally useful for large complex networks.

Therrien and Sudicky (1996) derived a model for a variably saturated fracture-matrix system having three dimensions in which advective fluid exchange is allowed between the fractures and matrix. A modified form of the Richards' equation was used for determining hydraulic head in the matrix, and an extension to the variably saturated flow equations was used for hydraulic head in the fracture. The fractures were idealized as two-dimensional parallel plates, and fluid leakage flux was used to link the equations for the fracture with that for the matrix. The resulting system of governing equations was solved using the control-volume finite-element method in conjunction with Newton–Raphson linearization. Although there is no technical limitation to the method in the simulation of flow in a nonorthogonal fracture system, as mentioned earlier, any nonorthogonal problem simulated using this model would be significantly limited in scale.

17.6.2 Solute Transport in a Discrete Fracture Network

Solute transport in fracture networks can be simulated in two ways: (1) using particle tracking, and (2) direct solution of the governing equations for solute transport. Of the two methods, the former has received more widespread use. In the following, both particle tracking and methods for direct solution will be described, with focus on the former.

In modeling solute transport in fracture networks, the presence of fracture intersections, where solute must be apportioned according to the flux entering and leaving the intersection node, must be incorporated. There are two approaches to this: (1) assume complete mixing at the node, and (2) use streamtube routing. For the former, concentration entering the intersection is assumed to completely mix, resulting in a uniform distribution of concentration leaving the intersection. For the latter, mass is distributed at the intersection according to the distribution of streamtubes, and no mixing is assumed to occur (Figure 17.30). Complete mixing at an intersection having incoming fractures is described by (Küpper et al., 1995a):

$$c = \frac{\sum_{i=1}^{n} c_i Q_i}{\sum_{i=1}^{n} Q_i} \qquad (26)$$

where c is the concentration in the intersection, and Q_i and c_i are the volumetric flux and concentrations in the incoming fractures, respectively. The development required for a rigorous implementation of streamtube routing is considerably more complex (e.g., Philip, 1988).

Berkowitz et al. (1994) suggested that diffusional transfer between streamtubes at intersections may smear the distinction between streamtubes, resulting in a distribution of concentration more like that observed with complete mixing. However, Küpper et al. (1995b) showed that, even in the absence of diffusion, for three of four possible flow conditions at intersections the complete mixing assumption and streamtube routing produce identical results. In addition, it was also shown that for some types of flow (i.e., radial flow in a network), the flow condition giving rise to the difference is rare. Thus, in practical terms, the degree of error introduced into a model by assuming complete mixing at every intersection is likely not significant. However, it is important to note that these concepts apply only to mixing at linked one-dimensional elements. In the more realistic case where two-dimensional planes intersect, the

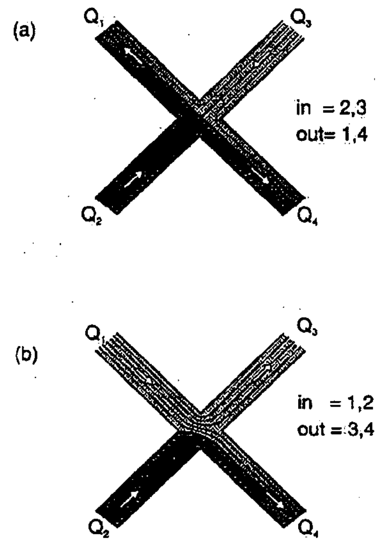

FIGURE 17.30 Schematic diagram showing mass transfer at a fracture intersection according to the distribution of streamtubes. (a) $Q_2 = Q_3$ and transport is split evenly into Q_1 and Q_4 and (b) $Q_1 > Q_2$ and transport is split unevenly between Q_3 and Q_4.

hydraulic head will be nonconstant along the intersection, resulting in much more complex mixing arrangements.

Particle tracking is a means to simulate solute transport by following the residence times of particles released into the flow system at a given boundary or internal location. In the most rudimentary implementation, a given number of particles, usually 20,000 to 30,000, are released into the flow system, routed at fracture intersections according to volumetric flux (i.e., assume perfect mixing at the intersection node) and eventually tracked to an exit boundary (Schwartz et al., 1983). The number of particles are summed at the exit boundary resulting in a breakthrough curve equivalent to a dirac input. Integration of the breakthrough curve with respect to time yields a breakthrough curve equivalent to a step-function input.

The use of particle tracking methods has been expanded in recent years to account for solute retardation (Dverstorp et al., 1992) and variable aperture fracture elements (Nordqvist et al., 1992). Retardation is accounted for by manipulating the travel time in individual fracture elements using the expression:

$$t_R = t_C R_a \tag{27}$$

where t_R is the travel time adjusted for sorption, t_C is determined from the cubic law, and R_a is as defined in Equation (12). Nordqvist et al. (1992) also manipulated residence time in fracture elements to account for the influence of variable aperture fractures. This was conducted by generating a spectrum of residence times using a variety of realizations of a variable aperture fracture having different mean apertures and different properties of the lognormal aperture distribution. To develop the residence time distribution for the system of linked linear elements, the residence time spectrum was randomly sampled for each fracture element (Figure 17.31). Matrix diffusion could also be accounted for in a similar fashion although the implementation would not be as rigorous as that achieved using the methods described in the following.

For two-dimensional networks of linked linear fracture elements, direct solution offers the most robust means of simulating transport in the fractures and interactions with the matrix. Sudicky and McLaren (1992) and Bogan (1996) describe finite-element and semianalytical approaches, respectively.

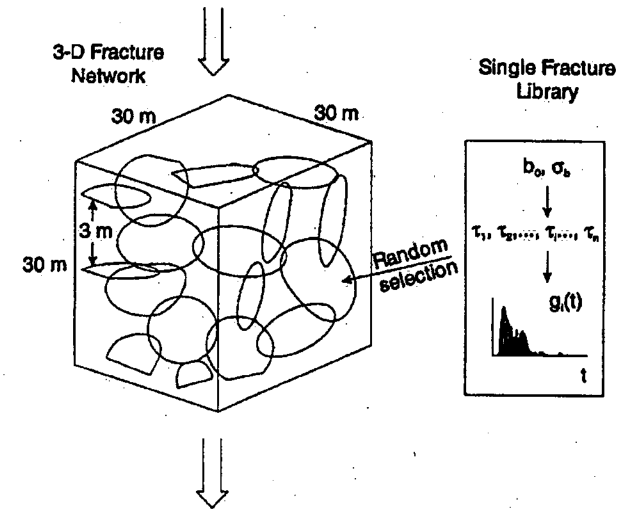

FIGURE 17.31 The incorporation of variable aperture fractures is introduced in a fracture network model. Here, b_o and σ_b are the two parameters describing the lognormal aperture distribution (mean aperture and standard deviation). The τ_i are effective transmissivities of the fractures in the library. The $g_i(t)$ plots are graphical illustrations of the residence time spectra for the fractures in the library. (From Nordqvist, A. W., Tsang, Y., Tsang, C.-F., Dverstorp, B., and Andersson, J. 1992. A variable aperture fracture network model for flow and transport in fractured rocks. *Water Resour. Res.* 28(6):1703-1713. With permission.)

The solution method described by Sudicky and McLaren (1992) accommodates advection-dispersion, retardation, and decay in the fracture and the same in the matrix. A third-type boundary condition is used for the exchange between fracture and matrix. This solution method can therefore simulate fractured domains having a permeable matrix (e.g., fractured clays). The finite element method is used to discretize the equations in the spatial coordinates, and the Laplace transform is used to manage the time derivative. To minimize the difficulties in discretization and to maximize the domain size for tractable problems, fracture geometry has been limited to orthogonal systems.

For two-dimensional networks having more random fracture orientations, the solution method of Bogan (1996) offers a practical alternative. In this case, only diffusive transport is allowed between the fracture and matrix. A semi-infinite domain is also defined for the diffusive transport in the matrix. Clearly, this is an approximation that is viable only for geological material having sparse fractures and low matrix porosity.

In three dimensions, the direct solution method of Therrien and Sudicky (1996) for a variably saturated fractured medium can be employed. The two governing equations for the fracture planes and matrix blocks are linked using continuity between the concentration in the fracture and that in the matrix at the fracture wall. Because the transport equations are linear, solution was based on a standard time-marching Galerkin scheme. Two-dimensional rectangular elements were used for the fractures, and three-dimensional rectangular prisms were used for the matrix.

Presently in the general practice of hydrogeology, the modeling of flow and transport in fractured rock systems is often conducted using EPM models. As we have suggested above, this approach will lead to error in the prediction of both groundwater flux or solute travel time, depending on the size of the domain modeled. At a domain scale of several hundreds of meters, or more, however, prediction of groundwater flux may be conducted with only minor error using EPM models, provided the characteristics of the major fracture zones and unfractured rock are known and appropriately represented. Thus, the hydraulic effects of short or long-term pumping or changes in boundary conditions such as recharge can be reliably explored using this approach.

Unfortunately, the prediction of solute transport using the EPM approach at this scale can be substantially erroneous. Thus, as a general rule of thumb, all predictions of contaminant transport and the design of remedial facilities at the scale of a contaminated site should be conducted using a model which, at minimum, incorporates multicontinuum concepts. In some cases, a defensible modeling strategy may be to simulate transport in the fracture system with simple analytical models which incorporate a parallel system of fractures and matrix diffusion. Although the fracture system may not be well represented by this approach, it is likely that this approach will lead to substantially more accurate predictions of contaminant transport than were employed in an EPM model.

For conditions where more accurate simulations of contaminant transport are required, such as for large-scale groundwater remediation programs or investigations of intrinsic bioremediation, there are now very robust modeling tools available which account for fractures on a discrete basis. Unfortunately, because few of these are widely available in commercial packages, attempts to conduct this type of modeling should be left to specialists.

Acknowledgment

We are grateful to this chapter's reviewer, Stephen Silliman, for many valuable and insightful comments.

For Further Information

Engelder et al. (1993) presents a thorough overview of the geological aspects of fracture mechanics and includes a comprehensive glossary of terms. de Marsily (1986) is a general text in quantitative hydrogeology which discusses flow and transport in fractures in an easy-to-follow manner. Kulander et al. (1990) discusses in detail core analysis and the identification and classification of breaks in rock core. Doe et al. (1987) discusses various techniques and strategies for hydraulic testing in fractured rock. Earlougher (1977) provides a comprehensive look at standard well-testing methods in the petroleum industry which can be adapted to hydrogeological investigations. Bear et al. (1993) provides a compilation of chapters investigating flow and contaminant transport in fractured rock, and in addition to theoretical discussions has sections on flow and solute transport in fracture networks.

References

Abelin, H., Birgersson, L., Gidlund, J., and Neretnicks, I. 1991. A large-scale flow and tracer experiment in granite 1. Experimental design and flow distribution. *Water Resour. Res.* 27(12):3107-3117.

Barenblatt, G. I., Zheltov, I. P., and Kochina, I. N. 1960. Basic concepts in the theory of seepage if homogeneous liquids in fissured rocks. *J. Appl. Math. Mech. Engl. Transl.* 24(5):852-864.

Barker, J. A. 1991. Reciprocity principle and analytical solution for Darcian flow in a network. *Water Resour. Res.* 27(5):743-746.

Bear, J. 1993. Modeling flow and contaminant transport in fractured rocks, in *Flow and Contaminant Transport in Fractured Rocks.* Eds. J. Bear, C.-F. Tsang, and G. de Marsily. Academic Press, San Diego, 1-37.

Bear, J. 1972. *Dynamics of Fluids in Porous Media.* Elsevier, New York.

Bear, J., Tsang, C.-F., and de Marsily, G. 1993. *Flow and Contaminant Transport in Fractured Rocks.* Academic Press, San Diego.

Berkowitz, B., Naumann, C., and Smith, L. 1994. Mass transfer at fracture intersections: an evaluation of mixing models. *Water Resour. Res.* 30(6):1765-1773.

Berkowitz, B., Bear, J., and Braester, C. 1988. Continuum models for contaminant transport in fractured porous formations. *Water Resour. Res.* 24(8):1225-1236.

Black, W. H., Smith, H. R., and Patton, F. D. 1987. Multiple-level groundwater monitoring with the MP system, in Proceedings NWWA-AGU Conf. Surface and Borehole Geophysical Methods and Groundwater Instrumentation, NWWA, Dublin, Ohio.

Bliss, J. C. and Rushton, K. R. 1984. The reliability of packer tests for estimating the hydraulic conductivity of aquifers. *Q. J. Engrg. Geol.*, 17:88-91.

Bogan, J. D. 1996. *A Semi-Analytical Model for the Simulation of Solute Transport in a Network of Fractures.* M.Sc. Thesis, University of New Brunswick, Fredericton NB.

Bredehoeft, J. D. and Papadopulos, S. S. 1980. A method for determining the hydraulic properties of tight formations. *Water Resour. Res.* 16(1):233-238.

Brown, S. R. 1995. Simple mathematical model of a rough fracture. *J. of Geophys. Res.* 100(B4):5941-5952.

Brown, S. R., Kranz, R. L., and Bonner, B. P. 1986. Correlation between the surfaces of natural rock joints. *Geophys. Res. Letters.* 13(13):1430-1433.

Cacas, M. C., Ledoux, E., de Marsily, G., Tillie, B., Barbareau, A., Calmels, P., Gaillard, B., and Margritta, R. 1990. Modelling fracture flow with a stochastic discrete fracture network: calibration and validation 1. The flow model. *Water Resour. Res.* 26(3):479-489.

Cherry, J. A. and Johnson, P. E. 1982. A multilevel device for hydraulic head monitoring and groundwater sampling in fractured rock. *Ground Water Monitoring Rev.* 2(3):41-44.

Cooper, H. H., Bredehoeft, J. D., and Papadopulos, I. S. 1967. Response to a finite diameter well to an instantaneous charge of water. *Water Resour. Res.* 3(1):263-269.

de Marsily, G. 1986. *Quantitative Hydrogeology.* Academic Press, Orlando, FL.

Doe, T. and Remer, J. 1980. Analysis of constant-head well tests in non-porous fractured rock, in *Third Invitational Well-Testing Symposium — Well Testing in Low Permeability Environments.* Berkeley, CA, 84-89.

Doe, T., Osnes, J., Kenrick, M., Geier, J., and Warner, S. 1987. Design of well testing programs for waste disposal in crystalline rock, in *Proceedings of 6th Congress of the International Society for Rock Mechanics.* Montreal, Canada.

Dougherty, D. E. and Babu, D. K. 1984. Flow to a partially penetrating well in a double porosity reservoir. *Water Resour. Res.* 20(8):1116-1122.

Drost, W., Klotz, D., Koch, A., Moser, H., Neumaier, F., and Werner, R. 1968. Point dilution methods of investigating ground water flow by means of radioisotopes, *Water Resourc. Res.* 4(1):125-146.

Dunnicliff, J. 1988. *Geotechnical Instrumentation for Monitoring Field Performance.* John Wiley & Sons, New York.

Dverstorp, B., Andersson, J., and Nordqvist, W. 1992. Discrete fracture network interpretation of field tracer migration in sparsely fractured rock. *Water Resour. Res.* 28(9):2327-2343.

Earlougher, R. C., Jr. 1977. *Advances in Well Test Analysis, Monogr. 5.* Society of Petroleum Engineers, Dallas, TX.

Elsworth, D. 1986. A model to evaluate the transient hydraulic response of three-dimensional sparsely-fractured rock masses. *Water Resour. Res.* 22(13):1809-1819.

Engelder, T., Fischer, M. P., and Gross, M. R. 1993. *Geological Aspects of Fracture Mechanics, A Short Course Manual.* Geological Society of America. Boulder, CO.

Faust, C. R. and Mercer, J. W. 1984. Evaluation of slug tests in wells containing a finite-thickness skin. *Water Resour. Res.* 20(4):504-506.

Gentier, S. and Billaux, D. 1989. Caracterisation en laboratoire de l'espace fissural d'une fracture, in *Proceedings of the International Symposium on Rock at Great Depth.* 1:425-431, A. A. Balkema, Rotterdam, The Netherlands.

Grisak, G. E., Merritt, W. F., and Williams, D. W. 1977. A fluoride borehole dilution apparatus for groundwater velocity measurements. *Can. Geotech. J.* 14:554-561.

Hakami, E. 1995. *Aperture Distribution of Rock Fractures,* Ph.D. Thesis, Department of Civil and Environmental Engineering, Royal Institute of Technology, Stockholm.

Hess, A. E. and Paillet, F. L. 1990. Applications of the thermal-pulse flowmeter in the hydraulic characterization of fractured rocks, in ASTM STP 1101:99-112.

Holst, T. B. 1982. Regional jointing in the northern Michigan basin. *Geology.* 10:273-277.

Holzhauser, G. R. 1989. Origins of sheet structure, 1. Morphology and boundary conditions. *Engineer. Geol.* 27:225-279.

Huyakorn, P. S., Lester, B. H., and Mercer, J. W. 1983. An efficient finite element technique for modeling transport in fractured porous media, 1. Single species transport. *Water Resour. Res.* 19(3):841-854.

Johns, R. A. and Roberts, P. V. 1991. A solute transport model for channelized flow in a fracture. *Water Resour. Res.* 27(8):1797-1808.

Jouanna, P. 1993. A summary of field test methods in fractured rocks, in *Flow and Contaminant Transport in Fractured Rocks.* Eds. J. Bear, C.-F. Tsang, and G. de Marsily. Academic Press, San Diego, 437-543.

Karasaki, K., Long, J. C. S., and Witherspoon, P. A. 1988. Analytical models of slug tests. *Water Resour. Res.* 24(1):115-126.

Kulander, B. R., Dean, S. L., and Ward, B. J. 1990. *Fractured Core Analysis: Interpretation, Logging and Use of Natural and Induced Fractures in Core: AAPG Methods in Exploration Series.* No. 8. American Association of Petroleum Geologists, Tulsa, OK.

Küpper, J. A., Schwartz, F. W., and Steffler, P. M. 1995a. A comparison of fracture mixing models, 1, A transfer function approach to mass transport modeling. *J. Cont. Hydrol.* 18:1-32.

Küpper, J. A., Schwartz, F. W., and Steffler, P. M. 1995b. A comparison of fracture mixing models, 2, Analysis of simulation trials. *J. Cont. Hydrol.* 18:33-58.

La Pointe, P. R. and Hudson, J. A. 1985. Characterization and interpretation of rock mass joint patterns. *Geological Society of America Special Paper 199.*

Lapcevic, P. A. 1997. *Tracer Experiments Conducted in a Discrete Horizontal Fracture Under Conditions of Forced Hydraulic Gradient and Natural Groundwater Flow,* M.Sc. Thesis, University of Waterloo, Waterloo, Ontario.

Lapcevic, P. A., Novakowski, K. S., and Cherry, J. A. 1990. The characterization of two discrete horizontal fractures in shale, in *Proc. Technology Transfer Conference, Ontario Ministry of Environment.* November, Toronto. Vol II, 486-495.

Lau, J. S. O. 1983. The determination of true orientations of fractures in rock cores. *Canadian Geotech. J.* 20:221-227.

Long, J. C. S., Gilmour, P., and Witherspoon, P. A. 1985. A model for steady fluid flow in random three-dimensional networks of disc-shaped fractures. *Water Resour. Res.* 21(8):1105-1115.

Moench, A. F. and Hsieh, P. A. 1985. Analysis of slug test data in a well with finite thickness skin, in *Memoirs of the 17th International Congress on the Hydrogeology of Rocks of Low Permeability,* 17:17-29, International Association of Hydrologists, Tucson, AZ.

Moreno, L., Tsang, Y. W., Tsang, C. F., Hale, F. V., and Neretnieks, I. 1988. Flow and tracer transport in a single fracture: a stochastic model and its relation to some field observations. *Water Resour. Res.* 24(12):2033-2048.

Neuzil, C. E. 1982. On conducting the modified 'slug' test in tight formations. *Water Resour. Res.* 18(2):439-441.

Nordqvist, A. W., Tsang, Y., Tsang, C.-F., Dverstorp, B., and Andersson, J. 1992. A variable aperture fracture network model for flow and transport in fractured rocks. *Water Resour. Res.* 28(6):1703-1713.

Novakowski, K. S. 1989. Analysis of pulse interference tests. *Water Resour. Res.* 25(11):2377-2387.

Novakowski, K. S. and Lapcevic P. A. 1994. Field measurement of radial solute transport in fractured rock. *Water Resour. Res.* 30(1):37-44.

Novakowski, K. S., Evans, G. V., Lever, D. A., and Raven, K. G. 1985. A field example of measuring hydrodynamic dispersion in a single fracture. *Water Resour. Res.* 21(8):1165-1174.

Odling, N. E. 1994. Natural rock profiles, fractal dimensions and joint roughness coefficients. *Rock Mech. Rock Engng.* 27(3):135-153.

Paillet, F. L. and Kapucu, K. 1989. Characterization of fracture permeability and fracture flow modeling at Mirror Lake, New Hampshire. *U.S. Geological Survey Water Resources Investigations Report* 89-4058. U.S. Government Printing Office. Denver, CO.

Philip, J. R. 1988. The fluid mechanics of fractures and other junctions. *Water Resour. Res.* 24(2):239-246.

Piggott, A. R. 1990. *Analytical and Experimental Studies of Rock Fracture Hydraulics.* Ph.D. thesis, Pennsylvania State University, University Park, PA.

Piggott, A., Moltyaner, G., Yamazaki, L., and Novakowski, K. 1997. Preliminary characterization of fracturing at the site of the Chalk River Laboratories, in *Proceedings of 50th Canadian Geotechnical Conference*, Ottawa, Canada (also NWRI No. 97-126).

Piggott, A. R., Huynh, T. N. T., Lapcevic, P. A., and Novakowski, K. S. 1996. Automated analysis of hydraulic and tracer tests conducted in fractured rock. *Hydrogeology J.* 4(3):84-93.

Piggott, A. R. and Elsworth, D. 1993. Laboratory assessment of the equivalent apertures of a rock fracture. *Geophys. Res. Letters.* 20(13):1387-1390.

Pyrak-Nolte, L. J., Myer, L. M., Cook, N. G. W., and Witherspoon, P. A. 1987. Hydraulic and mechanical properties of natural fractures in low permeability rock, in *Proceedings of 6th Congress of the International Society for Rock Mechanics*, Montreal, Canada, 225-231.

Ragan, D. M. 1973. *Structural Geology: An Introduction to Geometrical Techniques.* John Wiley & Sons, New York.

Raven, K. G. 1986. Hydraulic characterization of a small ground-water flow system in fractured monzononitic gneiss. *Nat. Hyd. Res. Inst. Scientific Series No. 149*, No. 30. Government of Canada, Ottawa.

Raven, K. G., Novakowski, K. S., and Lapcevic, P. A. 1988. Interpretation of field tracer tests of a single fracture using a transient solute storage model. *Water Resour. Res.* 24(12):2019-2032.

Rowe, R. K. and Booker, J. R. 1990. Contaminant migration through fractured till into an underlying aquifer. *Can. Geotech. J.* 27(4):484-495.

Sageev, A. 1986. Slug test analysis. *Water Resour. Res.* 22(8):1323-1333.

Sanford, B. V., Thompson, F. J., and McFall, G. H. 1985. Phanerozoic and recent tectonics of the Canadian Craton, in *The Geoscience Program — Proceedings of the Seventeenth Information Meeting of the Nuclear Fuel Waste Management Program*, Atomic Energy of Canada Limited, TR-299:334-352. Winnipeg.

Schwartz, F. W. and Smith, L. 1988. A continuum approach for modeling mass transport in fractured media. *Water Resour. Res.* 24(8):1360-1372.

Schwartz, F. W., Smith, L., and Crowe, A. 1983. A stochastic analysis of macroscopic dispersion in fractured media. *Water Resour. Res.* 19(5):1253-1265.

Shapiro, A. M. and Nicholas, J. R. 1989. Assessing the validity of the channel model of fracture aperture under field conditions. *Water Resour. Res.* 25(5):817-828.

Smith, L. and Schwartz, F. W. 1984. An analysis of the influence of fracture geometry on mass transport in fractured media. *Water Resour. Res.* 20(9):1241-1252.

Snow, D. T. 1969. Anisotropic permeability of fractured media. *Water Resour. Res.* 5(6):1273-1289.

Sudicky, E. A. 1990. The Laplace transform galerkin technique for efficient time-continuous solution of solute transport in double-porosity media. *Geoderma.* 46:209-232.

Sudicky, E. A. and McLaren, R. G. 1992. The Laplace transform Galerkin technique for large-scale simulation of mass transport in discretely fractured porous formations. *Water Resour. Res.* 28(2):499-514.

Sudicky, E. A. and Frind, E. O. 1982. Contaminant transport in fractured porous media: analytical solution for a system of parallel fractures. *Water Resour. Res.* 18(6):1634-1642.

Tang, D. H., Frind, E. O., and Sudicky, E. A. 1981. Contaminant transport in fractured porous media: analytical solution for a single fracture. *Water Resour. Res.* 17(3):555-564.

Therrien, R. and Sudicky, E. A. 1996. Three-dimensional analysis of variably-saturated flow and solute transport in discretely-fractured porous media. *J. of Cont. Hydrol.* 23(1-2):1-44.

Trainer, F. W. 1988. Hydrogeology of the plutonic and metamorphic rocks, in *Hydrogeology.* Eds. Back, W., Rosenshein, J. S., and Seaber, P. R. Geological Society of America, The Geology of North America, Boulder, CO, v. O-2:367-380.

Tsang, Y. W. 1984. The effect of tortuosity on fluid flow through a single fracture. *Water Resour. Res.* 20(9):1209-1215.

Tsang, Y. W. and Tsang, C. F. 1987. Channel model of flow through fractured media. *Water Resour. Res.* 23(3):467-479.

Tsang, Y. W. and Witherspoon, P. A. 1983. The dependence of fracture mechanical and fluid flow properties on fracture roughness and sample size. *J. of Geophys. Res.* 88(B3):2359-2366.

Vickers, B. C., Neuman, S. P., Sully, M. J., and Evans, D. D. 1992. Reconstruction and geostatistical analysis of multiscale fracture apertures in a large block of welded tuff. *Geophys. Res. Letters.* 19(10):1029-1032.

Wang, J. S. Y., Narasimhan, T. N., and Scholz, C. H. 1988. Aperture correlation of a fractal fracture. *J. Geophys. Res.* 93(B3):2216-2224.

Williams, H. R., Corkery, D., and Lorek, E. G. 1985. A study of joints and stress-relief buckles in Paleozoic rocks of the Niagara Peninsula, southern Ontario. *Can. Geotech. J.* 22:296-300.

Witherspoon, P. A., Wang, J. S. Y., Iwai, K., and Gale, J. E. 1980. Validity of cubic law for fluid flow in a deformable rock fracture. *Water Resour. Res.* 16(6):1016-1024.

Ziegler, T. W. 1976. *Determination of Rock Mass Permeability.* Waterways Experiment Station, Technical Report S-76-2, Vicksburg, Mississippi.

Zemanek, J., Caldwell, R. L., Glenn, E. E., Holcomb, S. V., Norton, L. J., and Strauss, A. J. D. 1969. The borehole televiewer — a new logging concept for fracture location and casing inspection. *J. Pet. Technol.* 21(12):762-774.

Glossary

Aperture Separation distance between two fracture surfaces; used as measure of fracture width.

Borehole Drilled open hole in rock. Boreholes may be of any orientation and plunge from vertical to horizontal in relation to the earth's surface.

Channel Preferred pathway in a single fracture plane or fracture network.

Conceptual Model Geological and/or hydrogeological image representing natural system.

Fracture Any planar or curviplanar discontinuity or break in a rock mass that has formed as a result of a brittle deformation process. Joints, shear fractures, faults, microcracks, etc., are all examples of fractures.

Fracture Network Two- or three-dimensional arrangement of intersecting fractures. Fractures in a network may be of identical aperture, length, or orientation or may be represent a distribution of fractures of varying parameters.

Hydraulic Test Test involving the injection or withdrawal of water into a given test zone to determine the permeability of the zone. Either the transient or steady-state response can be used.

Interference Test Hydraulic test conducted between two or more hydraulically connected zones. A vertical interference test can be conducted between two isolated zones in a single borehole.

Joint A mesoscopic fracture in rock exhibiting purely opening mode displacement, with no appreciable shear offset.

Matrix Diffusion Process whereby solute from water in fracture is transferred to water in the pore spaces of rock through chemical diffusion.

Rock Matrix Structure of unfractured bulk rock mass composed of mineral grains, cement, pore water, and pore space.

Sheeting Structure Mesoscopic fractures formed due to the vertical expansion of the rock resulting from erosional unloading. Sheeting structures are often found parallel to the earth's surface in all types of rock and are common conduits for groundwater flow at the regional scale.

Skin Zone around borehole which has different properties than the bulk rock mass. A positive skin suggests the permeability around the borehole is less than the bulk rock, whereas a negative skin suggests greater permeability. Skin zones may be caused by fracture infilling due to rock flour, drill bit damage, or invasion of drilling muds.

Surface Roughness Texture of fracture surface due to asperities in the plane. Roughness can range from smooth planes to highly irregular surfaces.

Wellbore Storage Volume of water in the borehole which, when pumping is initiated, is first depleted prior to water stored in fracture or rock matrix.

Environment Canada   Environnement Canada

Canada

Canada Centre for Inland Waters
P.O. Box 5050
867 Lakeshore Road
Burlington, Ontario
L7R 4A6 Canada

National Hydrology Research Centre
11 Innovation Boulevard
Saskatoon, Saskatchewan
S7N 3H5 Canada

St. Lawrence Centre
105 McGill Street
Montreal, Quebec
H2Y 2E7 Canada

Place Vincent Massey
351 St. Joseph Boulevard
Gatineau, Quebec
K1A 0H3 Canada

Centre canadien des eaux intérieures
Case postale 5050
867, chemin Lakeshore
Burlington (Ontario)
L7R 4A6 Canada

Centre national de recherche en hydrologie
11, boul. Innovation
Saskatoon (Saskatchewan)
S7N 3H5 Canada

Centre Saint-Laurent
105, rue McGill
Montréal (Québec)
H2Y 2E7 Canada

Place Vincent-Massey
351 boul. St-Joseph
Gatineau (Québec)
K1A 0H3 Canada